POLITECNICO DI TORINO

Master of Science in
Mechatronics Engineering

Master Thesis

Advanced Control Algorithm for Hydraulic Drive Systems

By

Wuyu Chen

Supervisor:
prof. Monika Ivantysynova
prof. Mazza Luigi

I would like to dedicate this thesis to my loving family

Acknowledgements

First and foremost, I would like to thank Professor Monika Ivantysynova for giving me an opportunity to be a visiting scholar in her research team in Maha Fluid Power Research Center as well as her supervision. Her constant support, patient guidance, assistance and encouragement have been of enormous importance to the completion of this dissertation. I greatly appreciate Professor Mazza Luigi and Professor Andrea Vacca offered me to conduct research in hydraulic fields.

This research could not have a possibility without the resources and help by several colleges in Maha. A special thanks to Pranay Banerjee and Ryan Jenkins for being great mentors, solving problems and brainstorming. I would cherish all knowledge learning from them. I am grateful to Susan Gauger, Ashkan Darbani for making me feel at home when I stayed at Lafayette. Finally, I would like to acknowledge and thank all my close friends at Purdue University and lab-mates for all the good times we spent in the United State.

Content

Nomenclature vi
Abbreviations ix
Abstract x
1. Introduction 1
1.1 Motivation 1
1.2 Hydraulic Power Propulsion System 2
1.2.1 Hydrostatic Transmission 3
1.2.2 Parallel Hydraulic Hybrids 3
1.2.3 Series Hydraulic Hybrids 4
1.2.4 Power-split Hydraulic Hybrids 5
1.3 Regenerative Brake 6
2. Maha Hydraulic Hybrid 8
2.1 Developing Process 8
2.2 Scheme and Operating Principle 9
2.3 Operation Mode 11
2.3.1 Non-hybrid Driving Mode 11
2.3.2 Hybrid Driving Mode 12
2.3.3 Regenerative Braking Mode 12
2.3.4 Coasting Mode 12
3. Mathematic Model for Maha HHV 13
3.1 One-dimensional Vehicle Model 13
3.2 Hydraulic Transmission 14
3.2.1 Hydraulic Pump and Motor 15
3.2.2 Bladder Accumulator 17
3.2.3 Check Valves, Relief Valves and Enabling Valve 19
4. Control Algorithm Development 20
4.1 Electronic Control and Data Acquisition System 20
4.2 Novel Torque Based Braking Control Strategies 21
4.2.1 Torque Mapping 22
4.2.2 Feedback Control 24
4.2.3 Feedforward Control 28
4.3 Supervisory Control 31

4.3.1 Supervisory Control for Brake 32
4.3.2 Supervisory Control for Acceleration 32
4.4 Simulation Result 33
4.5 Experimental Result 39
5. Summary and Future Work 42
References 45

Nomenclature

Symbol	Description	Unit SI
A_f	Frontal area	m^2
a	Acceleration rate	m/s^2
C_{acm}	Hydraulic capacitance of accumulator	Pa
C_d	Coefficient of aerodynamic drag	-
C_H	Hydraulic capacitance	Pa
C_r	Coefficient of rolling resistance	-
C_v	Coefficient of flow through the valve	-
E	Energy	J
e	Tracking error	-
$E_{capacity}$	Energy stored in high pressure accumulator	J
F_a	Force due to aerodynamic drag	N
F_b	Force due to braking	N
F_{bf}	Force due to braking on front axle	N
F_{br}	Force due to braking on rear axle	N
F_g	Force due to grade on the road	N
F_r	Force due to rolling resistance	N
F_{rf}	Force due to rolling resistance on front axle	N
F_{rr}	Force due to rolling resistance on rear axle	N
F_x	Tractive force	N
F_{xf}	Tractive force on front axle	N
F_{xr}	Tractive force on rear axle	N
g	Gravitational constant	m/s^2
i_{axle}	Gear ratio between drive-axle and units 2, 3	-
J	Inertial moment of vehicle	$kg \cdot m^2$
K_p	Coefficient for proportional term	-
K_i	Coefficient for integral term	-

Symbol	Description	Unit SI
K_d	Coefficient for derivative term	-
K_{oil}	Bulk modulus of hydraulic oil	10^9 Pa, N/m^2
m	Mass of vehicle	kg
n	Coefficient of polytrophic process	-
p	Pressure	Pa
p_A	Pressure of line A	Pa
p_{acm}	Pressure of accumulator	Pa
p_{HPA}	Pressure of high pressure accumulator	Pa
p_{HP}	Pressure of high pressure line	Pa
p_{LP}	Pressure of low pressure line	Pa
p_{lim}	Limited pressure of relief valve	Pa
p_{out}	Pressure at outlet of valve	Pa
Q	Flow	m^3/s
Q_{check}	Flow through check valve	m^3/s
Q_{relief}	Flow through relief valve	m^3/s
Q_{eff}	Effective flow	m^3/s
Q_s	Volumetric losses	m^3/s
$Q_{s,scaled}$	Scaled volumetric losses	m^3/s
Q_{th}	Theoretical flow	m^3/s
r_{wheel}	Rolling radius of wheel	m
T	Torque	$N \cdot m$
t	Time	$N \cdot m$
T_{23}	Torque derived from unit 2,3	$N \cdot m$
T_{cmd}	Command torque	$N \cdot m$
T_{sys}	System torque	$N \cdot m$
T_b	Braking torque	$N \cdot m$
T_r	Reference Torque	$N \cdot m$
T_s	Torque losses	$N \cdot m$

Symbol	Description	Unit SI
$T_{s,scaled}$	Scaled torque losses	$N \cdot m$
T_{th}	Theoretical torque	$N \cdot m$
u	Control input	-
V	Volume of hydraulic line	m^3
v	Velocity	m/s
V_0	Volume of accumulator at pre-charge pressure	m^3
V_i	Derived displacement volume of hydraulic unit	m^3
x	State	-
y	Control output	-
β	Percentage of displacement	%
ω	Rotation speed of hydraulic unit	rpm
ω_{wheel}	Rotation speed of wheel	rpm
ε	Ratio of energy recovery	%
ρ_A	Air density	kg/m^3
λ	Linear scaling factor	-
Δp	Differential pressure	Pa
η	Efficiency	-
η_{axle}	Drive-axle efficiency	-
θ	Angle	rad

Abbreviations

Symbol	Description
AASHTO	American Association of State Highway and Transportation Officials
AMC	American Motors Corporation
CAD	Computer Aided Design
cRio	Compact Reconfigurable Input Output
CVT	Continuously Variable Transmission
ECE R90	Electric World Forum for Harmonization of Vehicle Regulations
EHV	Electric Hybrid vehicle
EIA	Energy Information Administration
EV	Enabling Valve
EV_{HP}	Enabling Valve of High Pressure Accumulator
EV_{LP}	Enabling Valve of Low Pressure Accumulator
FPGA	Field-programmable Gate Array
FTA	Federal Transit Administration
HP	High Pressure
HPA	High Pressure Accumulator
HHV	Hydraulic Hybrid Vehicle
HST	Hydrostatic Transmission
ICE	Internal Combustion Engine
ISO	International Organization for Standardization
LA92	Unified Dynamometer Driving Schedule
LP	Low Pressure
NI	National Instruments
PGT	Planetary Gear Train
P-HHT	Parallel Hydraulic Hybrid Transmission
PID	Proportional, Integral, Derivative
PS-HHT	Power-split Hydraulic Hybrid Transmission
S-HHT	Series Hydraulic Hybrid Transmission
SOC	State of Charge
UDDS	Urban Dynamometer Driving Schedule

Abstract

With the enhancing awareness of environmental protection, energy conservation and emission reduction, there are a mushrooming number of advanced technologies coming along for improving fuel economy and reducing emission. Hydraulic hybrid as one of the promising methods has spurred renewed interest no matter on on-road or off-road vehicle fields because of its benefits over electrical technologies. A novel hydraulic hybrid configuration named Maha hydraulic hybrid which is different from electric and other types of hydraulic configuration combining advantages of both hydrostatic and series hybrid, requires a sequence of control strategies to realize its optimal potential, and to improve its drivability, performance, etc. A controller for regenerative braking and supervisory control systems for taking the control of charging or discharging high pressure accumulator have been designed.

The regenerative braking controller is to control displacement of hydraulic units to provide desired torque commanded by driver. Moreover, supervisory control methodologies not only monitor whether regenerative braking should be disable or not, but also govern switch-on or switch-off of high pressure enabling valve for deciding high pressure accumulator whether connected with hydraulic transmission. For evaluating the performance of those control algorithms, a driver model close-loop simulation based on physical features is established in the MATLAB/SIMMULINK environment. And then, a simple validation and verification in simulation by means of standard driving cycle have been introduced, including non-hybrid driving mode, hybrid driving mode and braking mode. The simulation result demonstrates that firstly, regenerative braking is satisfied with the overwhelming majority of braking requirements, whose energy recovery rate is up to 70%; secondly, under the control of novel torque-based controller, its braking performance and drivability are quite similar with original vehicle or even better; finally, transmission is available to switch driving mode between non-hybrid mode and hybrid mode automatically to utilize energy stored in high pressure accumulator as much as possible.

The feasibility of novel controller is further explored by implementing and testing it on Maha hydraulic hybrid vehicle with an on-road environment. Measurement results confirm the viability, drivability and driving performance of torque-based control strategies as well as supporting supervisory control.

1. Introduction

1.1 Motivation

With the increasing number of fossil fuels consuming, concerning the future of energy dilemma, and a rising awareness of environmental protection as well as the environmentally friendly society, all kinds of energy-saving technologies and approaches have been investigated and applied to reduce energy consumption and pollution emissions. There are many available solutions including, but not limited to reducing energy losses, increasing energy generation such as using renewable or clean energy sources, utilizing hybrid powertrain [1].

Although various advanced technologies and solutions are in use, the truth of the rapid depletion and the dependence of petroleum sources has not changed. According to the report from Energy Information Administration (EIA), **Figure 1.1** indicates that the usage of petroleum took up 37% of total energy consumption in the U.S.; in other words, petroleum still plays an important role in daily life [2]. **Figure 1.2** shows that transportation had contributed to the largest proportion of petroleum consumption and consumed over two thirds of the total petroleum production in the past few years. It is a remarkable fact that consumption of on-road vehicle such like cars and trucks was close to 85% of total transportation consumption indicated by **Figure 1.3** [3]. Therefore, to reduce or at lease minimize the rise of fossil fuel consumption, it is of great significance to improving the efficiency of transportation especially on-road vehicle.

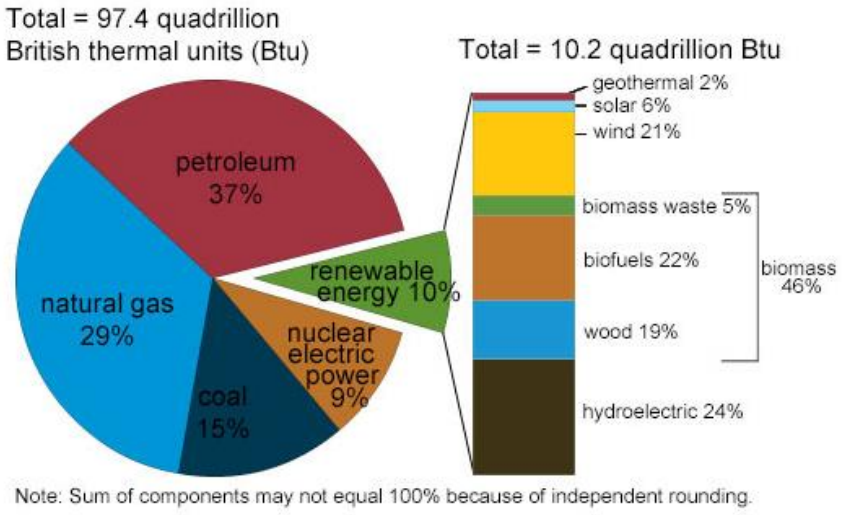

Figure 1.1: U.S. energy consumption by energy source, 2016 [2]

One of the most successful approach to improve vehicle efficiency is to hybridize powertrain. A hybrid road vehicle is one in which propulsion energy, during specified operational missions, is available from two or more kinds or types of energy, sources, or converters. At least one store device or converter must be on-board [4].Automobile industry, BMW and Toyota for example, has already focused on developing hybrid drives. Nowadays, hydraulic hybrid and electric hybrid are the two main hybrid technologies used in hybrid vehicles, but electric hybrids dominate on-road filed. However, hydraulic hybrid systems have several benefits such like less expensive and less weigh, due to price and weight of batteries required by electric systems. In 2012, according to the report of design and development series hydraulic hybrid

transit bus named LCO-I40H who was compared with conventional city busses and electric hybrid buses, U.S. Federal Transit Administration (FTA) reported that purchase price of LCO-I40H is 20% lower than that of most electric hybrids, and its lifecycle costs can be saved over 30%. Furthermore, it demonstrated that series hydraulic hybrid system has an over 30% higher efficiency than the best diesel-electric hybrid bus, and doubles the fuel economy in comparison with basic diesel buses [5]. Consequently, it is worthwhile to do research in hydraulic hybrid powertrain whether in theory research or practical application.

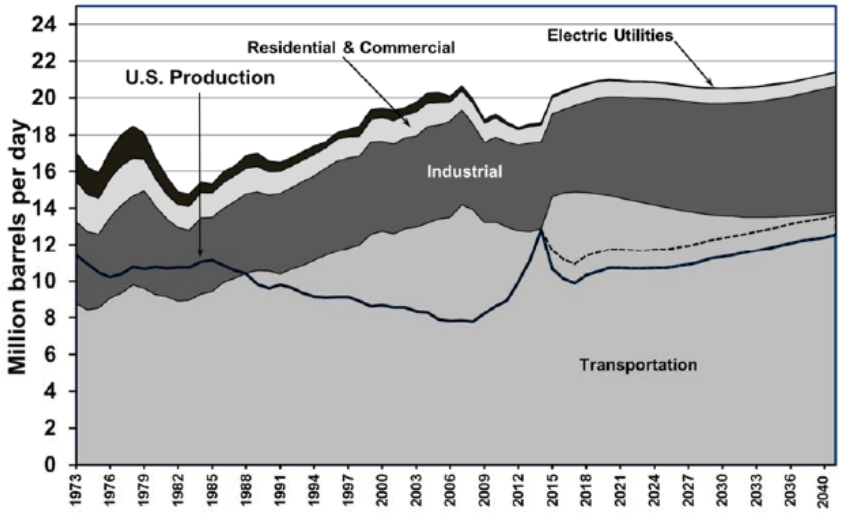

Figure 1.2: United States Petroleum Production and Consumption – All Sectors, 1973–2040 [3]

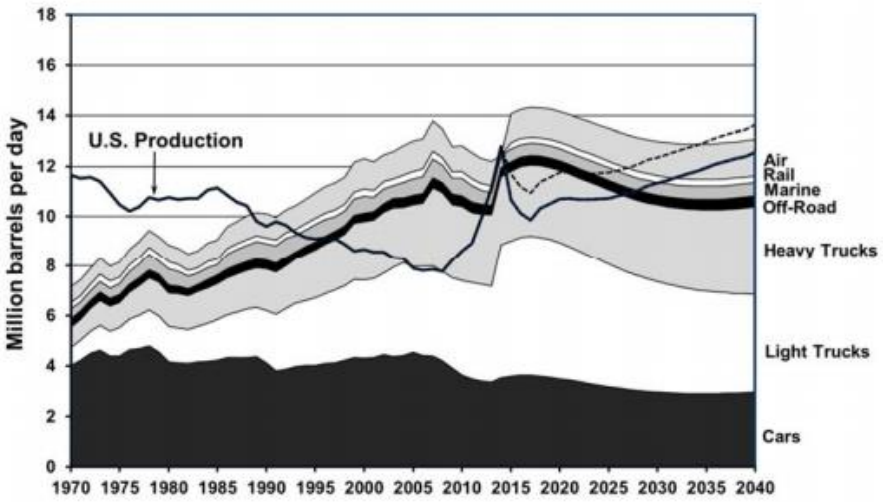

Figure 1.3: United States Petroleum Production and Transportation Consumption, 1970–2040 [3]

1.2 Hydraulic Power Propulsion System

The basic law of hydrostatics was first formulated by Blaise Pascal in 1647, but its application as a mean of automobile propulsion system had obtained notice unit 1993 [6]. There are several available types of hydraulic transmission architectures applied in the market, including non-hybrid and hybrid. For hybrid hydraulic propulsion system, series, parallel and power-split hybrids are the three main hybrid architectures. All of hydraulic hybrid system requires energy

storage system, pneumatic-hydraulic accumulator is employed in most cases. In contrast, for non-hybrid, hydrostatic transmission is widely used.

1.2.1 Hydrostatic Transmission

Hydrostatic transmissions (HST) is a closed loop architecture driven mechanism by means of hydraulic fluid medium to transmit power from power source. This first commercially available vehicles with a hydrostatic drive was the Linde "hydrocar" in 1995, after that HST jumped into popularity in off-highway filed especially for small tractors and crawlers [7].

HST architecture shown by **Figure 1.4**, is composed of at least two hydraulic units named primary unit which is connect to internal combustion engine (ICE), and secondary unit connected to the wheels. In order to make HST system work in a continuously variable transmission (CVT), at least one of these two units should be variable displacement unit. During acceleration, primary unit works as a pump, and secondary unit works as a hydraulic motor, to convert hydraulic energy into kinetic energy. Further backward movement, vehicle can go in reverse with reverse flow. In braking, secondary unit becomes pump and primary unit acts as motor. On account of closed circuit, flow from one unit is certain to pass through the other one associated with losses. While, flow rate passing units dependent on displacement and rotational speed. Accordingly, a non- simultaneous control method named sequential control, which means at a time, only the displacement of one hydraulic unit is controlled with the other maintaining full displacement, is employed in HST.

Compared with conventional sliding gear transmission, HST has some benefits: drive wheels locked together, various slow speed, infinite number of speeds forward and backward, etc. Indeed, what the most compelling advantage it has is easily shifted to keep power matched ideal efficiency under condition with various fluctuating loads.

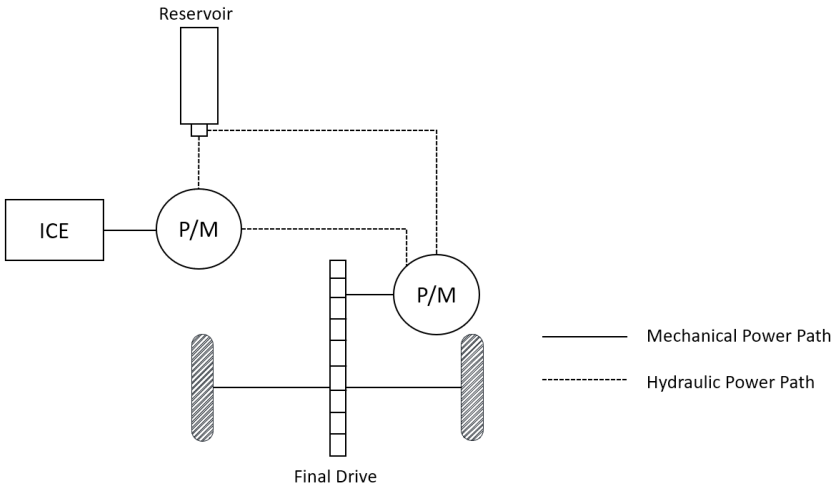

Figure 1.4: Hydrostatic Transmission Architecture

1.2.2 Parallel Hydraulic Hybrids

Parallel hybrid systems are the simplest since hydraulic part does not expect as a main power supply, and least costly type in current automotive use [8]. With the same idea of HST architecture, parallel hydraulic hybrid (P-HHT) shown in **Figure 1.5** have both an ICE and hydraulic motor that can individually drive the system or coupled up jointly driving system.

This system also requires a high pressure pneumatic-hydraulic accumulator for main energy storage and a low pressure accumulator for reservoir. Besides, hydraulic unit (pump/motor) is needed. Therefore, accumulator not only can absorb power and store it from existent transmission, and also release the energy it stored to drive the vehicle.

On the one hand, extra torque source from engine and kinetic energy from wheels during braking could be able to store in accumulator when hydraulic unit works as a pump, owing to an existence of discrete gears. On the other hand, when vehicle needs more power to accelerate or overcome resistance such like climbing, accumulator can provide supplementary energy to propel hydraulic unit while hydraulic unit runs as a motor. Those extra energy coming from excess torque supply as well as braking results, is able to reduce emissions and increase fuel efficiency.

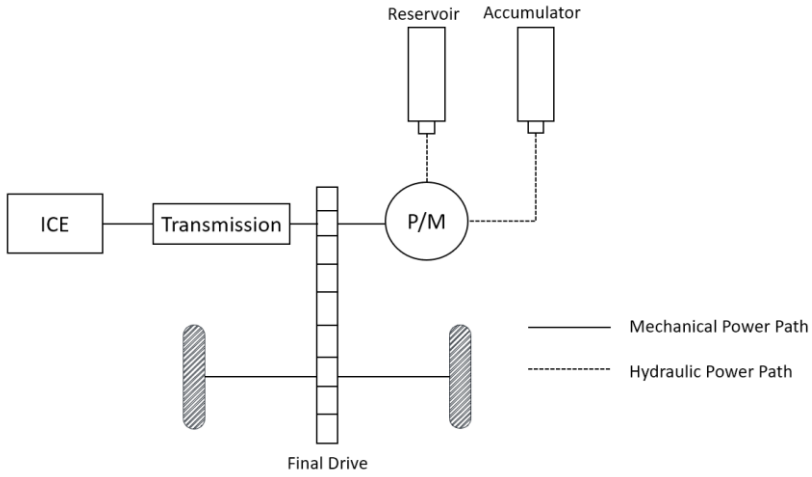

Figure 1.5: Parallel Hydraulic Hybrid Transmission Architecture

1.2.3 Series Hydraulic Hybrids

Series hydraulic hybrid (S-HHT) structure is no directly mechanical coupling between engine and wheels. Conventional Transmission between engine and wheels are removed as shown in **Figure 1.6**. This powertrain contains reservoir (low pressure accumulator), a high pressure accumulator as energy storage, hydraulic unit directly connected to the ICE, and another hydraulic unit as a reversible traction motor linked to a final drive. Different from P-HHT, hydraulic units in S-HHT are required to provide all of demanded power for any operating conditions.

During non-braking mode, primary unit as a pump converts engine power to fluid power, which is able to transmit fluid power either to secondary unit or accumulator. In addition, primary unit needs to maintain pressure in the lines. In the meantime, secondary unit is adjusted to meet required torque or speed. This operation mode is defined as secondary control mode. Furthermore, accumulator can collect energy through braking by means of regenerative brake.

This structure could be considered as hydrostatic transmission connected to a high pressure accumulator. So that system can work as CVT, and engine operating point can be independent of wheels speed. Most important, power management in S-HHT becomes flexible and engine can be downsized. In 2006, the unique UPS delivery truck was developed by several industry companies. In 2007, a report by U.S. Environmental Protection Agency (EPA) [9]demonstrated that this hydraulic hybrid UPS delivery vehicle saved 60% to 70% fuel and reduced emissions

up to 40%. Later, series hydraulic hybrid transit bus named LCO-I40H had a 109% improvement in fuel economy over the conventional one in 2012 [5].

S-HHT structure also has some drawbacks. It is well known that hydraulic pump and motor are in most efficient when they operate at high displacement and low pressure. Given that power of units is related to pressure difference across units and pressure in this system is predefined, both critical condition like low state-of-charge (SOC) in the accumulator and the capability for capturing energy during aggressive braking should be considered when sizing all of the hydraulic components. However, pressure in system is determined by high pressure accumulator, in a high pressure with low torque required condition, efficiency should be compromised.

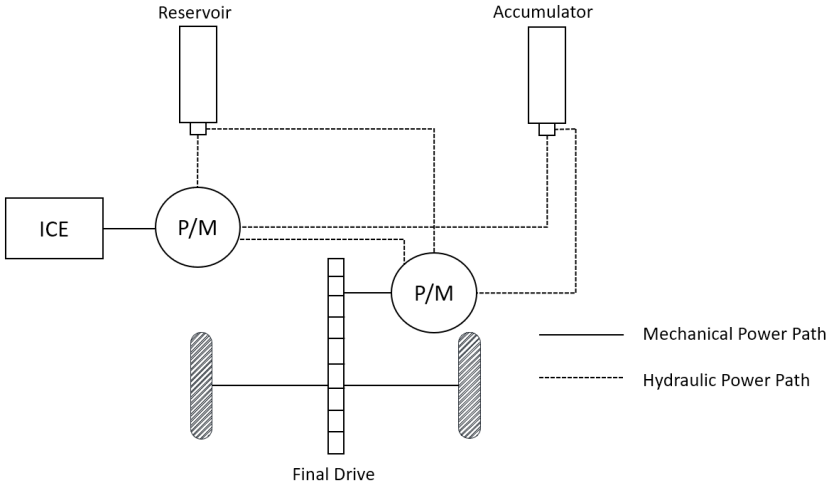

Figure 1.6: Series Hydraulic Hybrid Transmission Architecture

1.2.4 Power-split Hydraulic Hybrids

Power-split hydraulic hybrid (PS-HHT) is also known as series-parallel hydraulic hybrid, which attempts to make a combination of the decent characteristic of series hybrids and mechanical systems. Power-split structure can be categorized as input-coupled and output-coupled regarding diverse location of the planetary gear train (PGT). An output-couple configuration is shown in **Figure 1.7**.

The crucial working principle of PS-HHT is to decouple the power supply by means of PGT. As the heart of PS-HHT, PGT attaches to an engine and hydraulic units to split power between an effective mechanical part and flexible hybrid part, allowing optimizing engine efficiency, regenerative braking, and managing power flexibly. This transmission can act like a S-HHT when all the power is only coming from hydraulic part, act like P-HHT as well when power is combined. Before designed velocity, vehicle is driven by hydraulic part only, whose power is received from engine and accumulator. Along with increasing velocity, power through mechanical path will be increased until reaching designed velocity, whereas the power transmitted from hydraulic path will be reduced by tuning displacement of hydraulic pump. Its chief goal is to keep engine operating nearby the most efficient point with near-constant speed whatever in acceleration or cruise. Also, accumulator can be stored kinetic energy during braking when units go over-center.

Although power-split architecture and its applications have been flooding in electric hybrid filed, Lexus RX400h and Toyota Prius for example, hydro-mechanical transmission design

offers multiple advantages, analogous to already demonstrated benefits of electro-mechanical power-split drivelines, and this is likely to stimulate significant development efforts in the future [10].

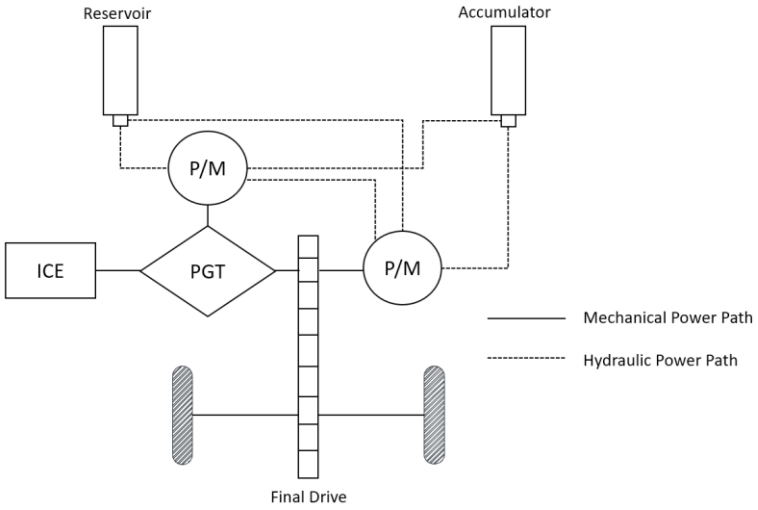

Figure 1.7: Power-split Hydraulic Hybrid Transmission

1.3 Regenerative Brake

The idea of energy regeneration brake came up in 1908 by C.J. Paulson and developed by American Motors Corporation (AMC) in 1967. Afterwards, it was commercialized by Japanese and Ford & Chevrolet licensed it from Toyota for manufacturing their hybrid vehicle [11].

The capability of capturing and reusing wasted braking energy during driving cycle is one of the most merit of implementing hybrid propulsion system. For example, in typical urban driving cycles such as LA92, New York City, the percentage of braking energy to traction energy are 58.01 percent and 81.9 percent respectively [12]. In conventional braking system, kinetic energy as well as gravity potential energy is transmitted into heat by friction brake when driver wants to slow or stop vehicle. On the contrary, regenerative brake has a capability of not only recovering energy by converting kinetic energy into another form of energy such as chemical energy stored in the battery or pneumatic-hydraulic energy stored in accumulator which is supposed to not only be used later to help propel the vehicle as extra sources, but also attends to slow or stop the vehicle.

There are diverse kinds of storage media are used to store recovered energy during braking. Power density and energy density are regarded as critical parameters for different energy storage media, which is classified by a Ragone Diagram [13] shown in **Figure 1.8**. **Figure 1.8** shows that hydraulic bladder accumulators have high power density and low energy density versus electric energy storage systems with low power density and high energy density. In other words, electric energy storage systems can store energy for a long time owing to its higher energy density in comparison of hydraulic one. But, because of a high power dense in hydraulic energy storage systems, it is able to recover braking energy as much as possible in a short interval with a fast rate. This typical advantage of hydraulic media makes hydraulic hybrids becomes more attractive than electric ones especially in a vehicle with a stop-and-go (regularly braking pattern) driving cycle such like delivery truck and city bus.

Because electric hybrid vehicles (EHV) dominate the market of on-road hybrid vehicle, almost the present research about regenerative braking are contributed to electric field. A variety of control strategies for regenerative braking system, such like fuzzy control to obtain decent braking performance and regenerative efficiency [14], advance control algorithm to enhance vehicle stability and fuel economy in co-operation braking mode [15], ECE R90 based control strategy in simulation and analysis of regenerative brake for P-HHV [16] have been carried out. In spite of this, a minority of literatures were related to regenerative braking in hydraulic hybrids.

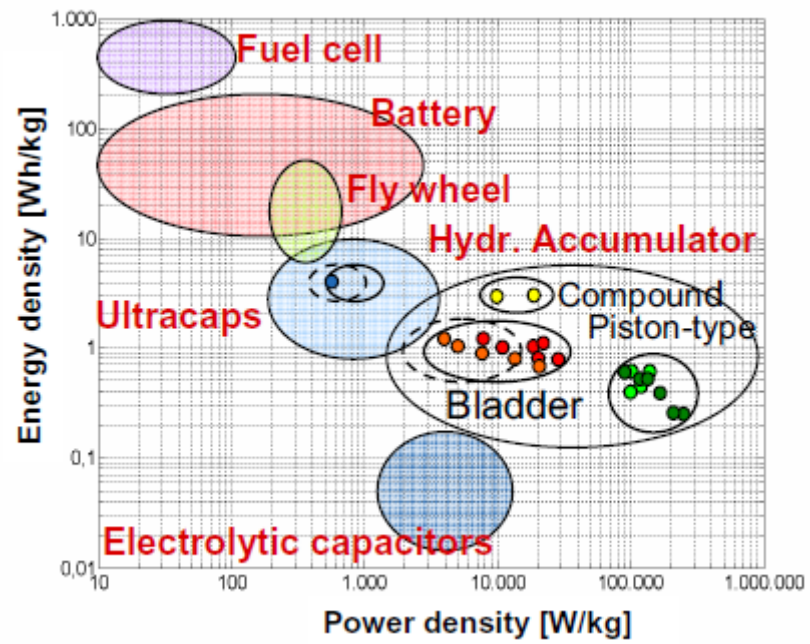

Figure 1.8: Ragone Diagram [13]

This paper will be devoted to developing control strategies for hydraulic hybrid vehicle (HHV) particularly to improve braking performance as well as driving comfort in regenerative braking part, and creating supervisory control logics for managing high pressure accumulator.

2. Maha Hydraulic Hybrid

2.1 Developing Process

Maha hydraulic hybrid, also called blended hybrid structure is defined as a powertrain with a combination of series hybrid and hydrostatic, operating in diverse modes to reach decent efficiency, which was first announced and investigated by Dr. Sprengel and Dr. Ivantysynova at the Maha Fluid Power Research Center in 2012 [17]. Afterwards, in order to compare an automatic transmission with Maha hydraulic hybrid, an optimum methodology was employed to control each transmission for a class II pickup truck under UDDS cycle. The result demonstrated that blended hybrid achieved 37% increase in fuel economy in comparison of automatic transmission [18]. Furthermore, these researchers had implemented a more complex transmission including blended hybrid as well as series hybrid to be the hydraulic path of power-split transmission correspondingly, to perform a more in-depth discussion of energetic analysis with various transmissions, whose consequences can be illustrated in **Table 2.1** [19]. We can make a conclusion that apart from complex power-split propulsion system, the blended hybrid which has the advantages of both HST and S-HHT, is the best choice in all categories of transmissions. Then, a hardware in the loop test rig which consists of Sauer S90 42cc/rev as hydraulic pumps/motors and 20L hydraulic bladder accumulator, was deigned to verify simulation result and test control strategy in an attempt to simulate a passenger vehicle[20].

Table 2.1 Fuel Economy and Energy Consumption of Various Transmissions [19]

Transmission	Fuel Economy (l/100 km)	Fuel Economy (mpg)	Engine Energy Generation (MJ)
Automatic	9.01	26.11	11.14
Automatic (no lockup clutch)	11.37	20.68	13.37
Manual	8.12	28.96	9.38
Series Hybrid	8.09	29.07	11.28
Blended Hybrid	8.02	29.34	10.58
Series Hybrid PST	7.77	30.28	10.55
Blended Hybrid PST	7.68	30.64	9.28

Above all explorations, they are able to prove that Maha hydraulic hybrid can be implemented in practice. After that, an adapted blended hybrid architecture for all-wheel drive (AWD) was designed. In the meantime, a series of complex reforming procedure containing but not only parameters investigation, sizing hydraulic components including static sizing and dynamic sizing by means of dynamic programming, pre-packaging on AutoCAD and installation on vehicle had been underway. Then blended hydraulic hybrid architecture was implemented on 1999 Range Rover 4.0SE built by Land Rover with a 4.0-liter, V-8 engine and all time four-wheel drive [21]. Besides, accessory systems such like a data acquisition and relevant control stagey based on MATLAB/SIMULINK and LabVIEW-National Instruments were instituted in this application platform shown in **Figure 2.1** [22]. So far, Maha hydraulic

hybrid vehicle (Maha HHV) was born. A number of critical parameters of Maha HHV are displayed in **Table 2.2**.

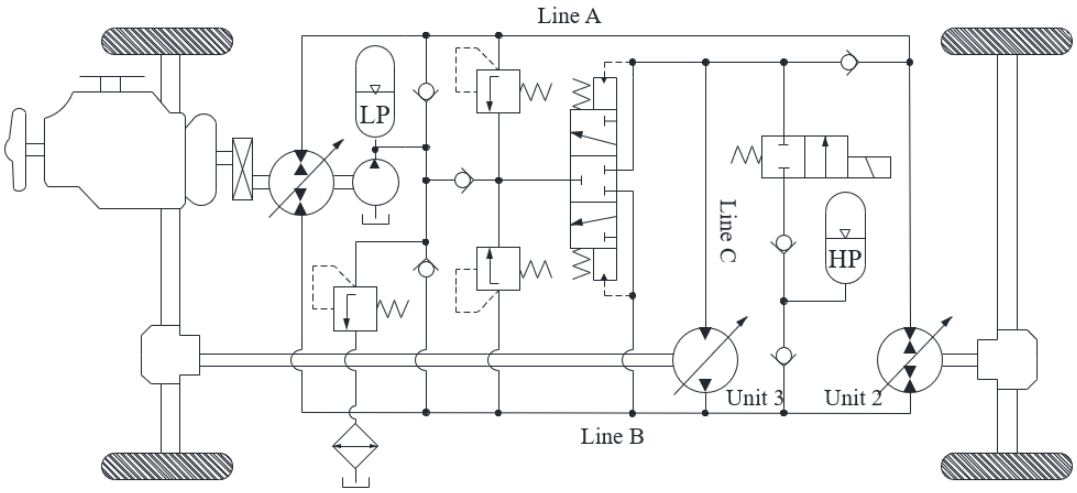

Figure 2.1: Mode-Switching Hybrid for AWD

Table 2.2 Parameters of Maha HHV

Parameter	Value
Max Power	320 kW @ 2600 RPM
Max Torque	142 Nm @ 4750 RPM
Gross Vehicle Mass	2780 kg
Drive-Axle Ratio	3.54:1
Rolling Radius	0.358 m
Front Area	2.78 m^2
Aerodynamic Drag	0.4
Rolling Resistance	0.022
Fuel	Gasoline

2.2 Scheme and Operating Principle

Maha hydraulic hybrid brings about a sustainable development in hardware, the latest architecture is illustrated in **Figure 2.2**, and parameters of main components are displayed in **Table 2.3**. In comparison with above-mentioned version shown by **Figure 2.1**, what the biggest modification is that an enabling valve (14) of low pressure accumulator (LPA) is added after the outlet of LPA, whose function is to avoid needless leakage when whole system is in static state, beyond that it must keep open.

This system has three hydraulic units named unit 1 (1), unit 2 (2), unit 3 (3) individually. Unit 1 is coupled with a gear box (18) which is linked to internal combustion engine (5) and charge pump (4). The main duty of unit 1 is to convert kinetic energy from ICE into hydraulic power to drive unit 2 and unit 3 in acceleration. Since this transmission is intended for a full-time

four-wheel drive, not only unit 2 is connected to rear axle and unit 3 is connected to front axle, but also both units are deliberated on same size. Moreover, charge pump (4) supplies flow to low pressure line by means of absorbing hydraulic oil from tank (9) and it also provides flow along with LPA (6) while unit 2 and unit 3 operate as pump for braking and energy storing. Another function of LPA is to reduce fluctuation owing to its high capacitance in hydraulic circuit, whose principle is quite similar with a high capacitor in an electric circuit. High pressure accumulator (HPA) (13) should be utilized only in hybrid mode or braking. The reason why a HPA enabling valve (13) linked with HPA is to control the working mode of transmission in either hydrostatic mode when HP enabling valve is close, or hybrid mode when HPA enabling valve is open. Apart from this, several check valves (8) should participate in, but their feature is not limited to classify operating mode. It is noteworthy that during braking, HPA enabling valve should remain closed so that HPA can absorbed flow from hydraulic units through the check valve.

Cooler (10) and flushing valve (15) are pretty important in closed circuit. Fluid apart from losses and internal leakage, flows from the motor outlet flows directly to pump inlet. If the transmission is in heavy load condition without cooler and flushing valve, overheat may produce owing to fluid circulating in the loop. The functionality of flushing valve is to exchange the fluid in the reservoir which is linked to cooler, with that in the loop when the transmission is operated in either forward or reverse. Oil which has been cooled from the reservoir will be charged by charge pump to the low pressure line, being the flow of the inlet of unit 1, or unit 2 as well as unit 3. Last but not the least, for safety reason, HP relief valves (11) and LP relief valves (12) are set up to 450 bar and 28 bar respectively.

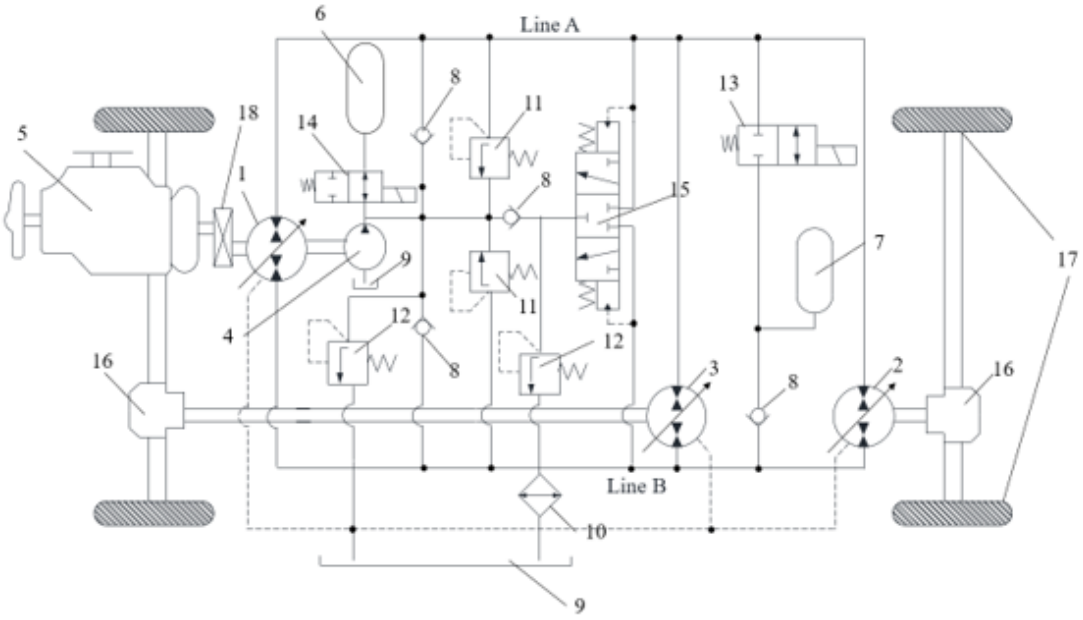

1. Unit1
2. Unit 2
3. Unit 3
4. Charge Pump
5. Combustion Engine
6. LP Accumulator
7. HP Accumulator
8. Check Valve
9. Reservoir
10. Oil Cooler
11. HP Relief Valve
12. LP Relief Valve
13. HPA Enabling Valve
14. LPA Enabling Valve
15. Flushing Valve
16. Drive-axle
17. Wheels
18. Gear Box

Figure 2.2: Maha Hydraulic Hybrid Transmission

Table 2.3: Parameters of Main Components in Maha HHV

Component	Size	Max Pressure	Max Speed	Pre-charge Pressure
Unit 1	100 cc/rev	450 bar	3650 rpm	-
Unit 2 and Unit 3	75 cc/rev	450 bar	3950 rpm	-
Charge Pump	26.4 cc/rev	210 bar	2500 rpm	-
LPA	42 L	350 bar	-	14.5 bar
HPA	32 L	500 bar	-	155 bar

2.3 Operation Mode

2.3.1 Non-hybrid Driving Mode

Non-hybrid driving mode containing forward driving and reverse driving, can be regarded as a hydrostatic mode when enabling valve (13) is closed. As similar HST, unit 1 is set to zero displacement while both unit 2 and unit 3 are at full displacement at the beginning. With the raising velocity and unit 1 displacement, pressure in line A keeps going up as a consequence of the flow providing by unit 1whereas other units absorb the flow. But pressure in the line would not raise without bound, it should meet the required torque depending on the load on wheels, and the motors displacements. Once unit1 has reached 100% displacement, in an effort to rise speed, displacement of unit 2 and unit 3 must be reduced. After this inflection point, unit 1 acts as a fixed displacement hydraulic pump and unit 2 and 3 operates as a variable displacement hydraulic motor, which is counter to the initial condition. As the mention of 1.2.1, this control method presented in **Figure 2.3**, which merely the displacement of one unit is adjusted with the others maintaining in full displacement, is defined as sequential control.

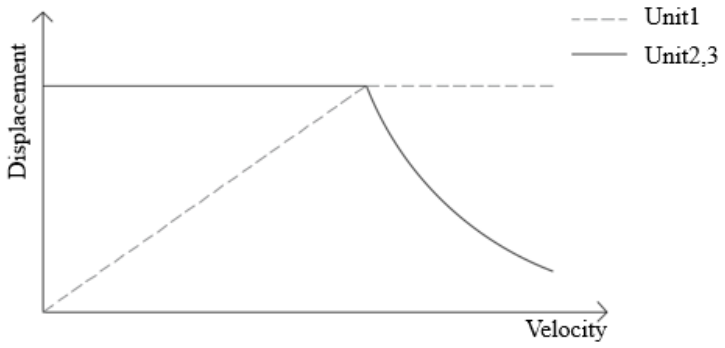

Figure 2.3: A Schematic of Sequential Control

Both unit 2 and unit 3 whether go over-center or not is the key point of the distinction between forward driving and reverse driving. When wheels go backwards, line A becomes high pressure line as before, whose required flow is pumping from unit 1, and propels vehicle moving as a result of the torque provided by unit 2 as well as unit 3. As a matter of fact, to make unit 1 goes over-center is another substitute for reverse driving. What I would like to stress is that the above method the vehicle have applied could be the optimal solution because the alternate is not

capable to capture energy during braking even though it is compelling in case of heavy and off-road vehicles.

2.3.2 Hybrid Driving Mode

When high pressure accumulator (7) is connected to line A with opening the enabling valve of HPA, system has to operate as a series hybrid transmission. In this case, flow going into line A is not only derived from hydraulic pump (1), but also getting from HPA. Therefore, pneumatic-hydraulic power stored in HPA can co-operate with the fluid power from unit 1 to provide enough torque required by hydraulic motors (2) and (3). A totally different control method from sequential control, named secondary control should be employed to handle this extra energy coming from HPA in hybrid driving mode. Under secondary control, the responsibility of unit 1 is only to monitor the line pressure to match the requirement of pressure by pumping flow from low pressure line to high pressure line; meanwhile, unit 2 as well as unit 3 are controlled to meet the required torque of which is a function consists pressure and displacement, with the help of changing its displacement.

However, it has numbers of criteria for Maha hydraulic hybrid system switching from non-hybrid mode to hybrid mode. First of all, the pressure of HPA should be higher than its pre-charge pressure; additionally, the pressure of line A should be close to the state-of-charge of HPA; last but not the least, vehicle should run over particular velocity to improve drive comfort at the moment in which HPA is connected.

2.3.3 Regenerative Braking Mode

In the cause of maximizing recovery rate of energy, neither hydrostatic braking nor friction brake are in use. It is opposite to non-hybrid and hybrid mode, unit 2 and unit 3 serve as a pump instead of motor to pressurize line B and charge HPA by pumping flow from tank and LPA, which saves energy by converting kinetic energy to pneumatic-hydraulic energy stored in HPA. This energy reserved in HPA is possible to be an extra boost power in next acceleration cycle. In this mode, the displacement of hydraulic unit is under control through brake pedal travel while unit 1 keeps zero displacement. Braking torque depends on firstly the differential pressure between inlet and outlet of pumps, displacement of units as well. However, if HPA is full, superfluous flow will only pass through HP relief valve (11) which is connected to line B, going back to reservoir rather than other approaches, drain line of those units for instance.

2.3.4 Coasting Mode

When either acceleration pedal or brake pedal is not as input for vehicle, there is no torque being supplied to the wheels through transmission; therefore, system operates at coasting mode with zero displacements of all hydraulic units as well as disconnection between HPA and line. Moreover, vehicle decelerates as a consequence of resistive forces, whose deceleration rate is supposed to be lower than braking.

3. Mathematic Model for Maha HHV

3.1 One-dimensional Vehicle Model

Given that as much of works focus on developing control system for hydraulic transmission rather than vehicle dynamics, a one-dimensional vehicle including neither suspension dynamics or tire dynamics called the modified double-corner model [23] is applied for modelling vehicle dynamics, which can demonstrate the longitudinal dynamics of the range rover shown in **Figure 3.1**.

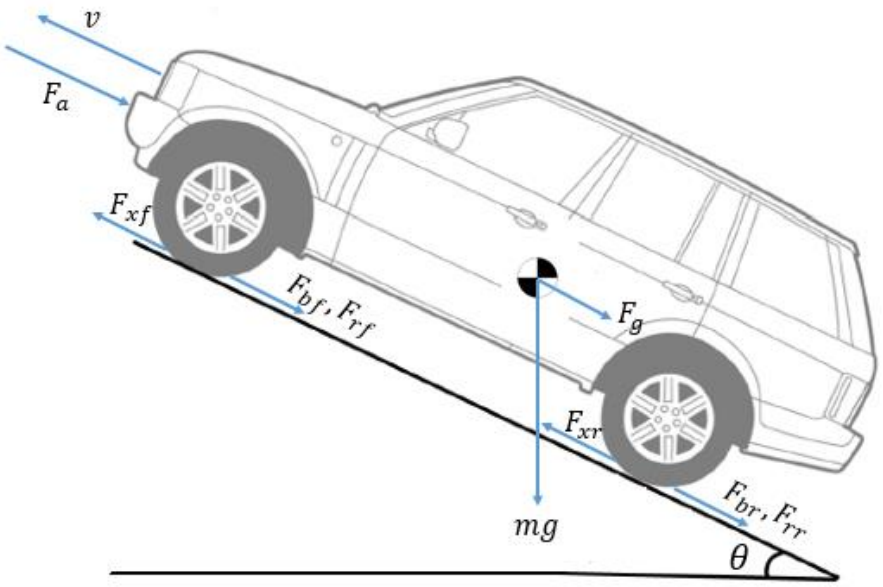

Figure 3.1: Force Analysis on Vehicle

According to Newton's second law, force balance with neglected lateral forces in vehicle dynamics can be expressed by Equation (3.1), including force provided by drive-axle derived from hydraulic system F_x, aerodynamic drag F_a, grading force F_g, rolling resistance F_r, and braking force F_b. The force or torque applied on the wheel given by Equation (3.2) from hydraulic system has to overcome the resistive forces to drive the vehicle, where F_{xf} and F_{xr} are forces working on front and rear wheels separately, T_{23} is torque provided by units 2 and 3, i_{axle} is the drive-axle ratio, η_{axle} is the efficiency of drive-axle, r_{wheel} is rolling radius of wheels obtained from **Table 2.2**. After that, vehicle speed as well as wheel speed can be calculated easily as in Equation (3.3). Since lateral forces are ignored, both wheel slip angle and body side slip angle are excluded in this research.

$$m\frac{dv(t)}{dt} = F_x - F_a - F_g - F_r - F_b \tag{3.1}$$

$$F_x = F_{xf} + F_{xr} = (T_{23} \cdot i_{axle} \cdot \eta_{axle})/r_{wheel} \tag{3.2}$$

$$\omega_{wheel}(t) = \frac{1}{r_{wheel}} \int \frac{F_x - F_a - F_g - F_r - F_b}{m} dt \tag{3.3}$$

Resistive forces can be illustrated by Equation (3.4), Equation (3.5) and Equation (3.6) [24]. Where, ρ_A, A_f, C_d, C_r and g are constant named air density, frontal area of the vehicle, factor of drag, factor of rolling resistance and gravitational acceleration respectively; m is the mass of vehicle; v is the vehicle velocity. In Equation (3.7), F_{bf} and F_{br} are braking forces on the front wheels and rear wheels independently; T_b is braking torque as a result of units 2 and 3.

$$F_a = \frac{1}{2}\rho_A A_f C_d v^2 \tag{3.4}$$

$$F_g = mg \sin\theta \tag{3.5}$$

$$F_r = F_{rf} + F_{rr} = mgC_r \cos\theta \tag{3.6}$$

$$F_b = F_{bf} + F_{br} = (T_b \cdot i_{axle} \cdot \eta_{axle})/r_{wheel} \tag{3.7}$$

It should be noted that hydraulic transmission can neither act on accelerating condition nor braking condition in the same time, whether forward drive or backward drive. Hence, F_b should be zero during acceleration; on the contrast, F_x should be zero during brake. Moreover, both F_x and F_b have a possibility to be zero during coasting.

3.2 Hydraulic Transmission

The whole hydraulic transmission operates as a result of the pressure built in the lines. Those pressure in the lines are a consequence of hydraulic flow coming in and out from hydraulic components connected to the lines, which is given by pressure built up equation as Equation (3.8). In Equation (3.10), a computation method of bulk modulus of hydraulic oil is given.

$$\dot{p} = \frac{1}{C_H} \sum Q \tag{3.8}$$

$$C_H = \frac{V}{K_{oil}} \tag{3.9}$$

$$K_{oil}(p) = (p + b)[\frac{1}{a} - \ln\left(1 + \frac{p}{b}\right)] \tag{3.10}$$

where

- p is the pressure in the line
- C_H is the hydraulic capacitance
- $\sum Q$ is the sum of inflow and outflow in the line
- V is the volume of the line
- K_{oil} is the oil's bulk modulus
- a = 0.0733 for HLP32 at 52℃ (20 cSt)
- b = 999.93 bar for HLP32 at 52℃ (20 cSt)

In order to obtain dynamic inflow as well as outflow of each hydraulic component, following parts in this chapter will be contributed to illustrate the model of hydrostatic transmission.

3.2.1 Hydraulic Pump and Motor

Hydraulic pump and motor which are axial piston machines in this case, work as heart in hydraulic transmission for making hydraulic flow be cyclic to produce torque to drive mechanical system. According to its functionality in circuit, equations about computing theoretical flow and theoretical torque are supposed to be its mathematic model given by Equation (3.11) and Equation (3.12) respectively. However, both flow and torque losses exist in real world, which should have effect on efficiency of hydraulic units. To gather the information of actual machine losses in operating conditions, measurements under steady-state conditions with a broad range of differential pressures, rotation speeds and relative displacements had been made [25]. Highly non-linear hydraulic unit loss models by empirical relation are given by Equation (3.13) and Equation (3.14) [26].

$$Q_{th} = \beta \cdot \omega \cdot V_i \tag{3.11}$$

$$T_{th} = \frac{\beta \cdot \Delta p \cdot V_i}{2\pi} \tag{3.12}$$

$$Q_s = f_Q(\Delta p, \omega, \beta) \tag{3.13}$$

$$T_s = f_T(\Delta p, \omega, \beta) \tag{3.14}$$

where

- $\mathrm{Q_{th}}$ and $\mathrm{Q_s}$ are theoretical flow and flow losses respectively
- $\mathrm{T_{th}}$ and $\mathrm{T_s}$ are theretical torque and torque losses respecitvely
- β is percentage of displacement of axial pistion device
- ω is rotation speed of axial pistion device
- $\mathrm{V_i}$ is the derived displacement of axial pistion device
- $\Delta \mathrm{p} = \mathrm{p_A} - \mathrm{p_B}$ is the different pressure between entrance and exit of axial pistion device

Unfortunately, these steady-state measurements are only evaluated on typical axial piston machine, and it is not reality to measure these losses in all sizes. Therefore, linear scaling laws given by Equation (3.16) and Equation (3.17) among scaling factor λ are employed to calculate losses of hydraulic units of diverse sizes. Scaling factor λ can be found in Equation (3.15), where $\mathrm{V_{scaled}}$ is the scaled (desired) displacements, and $\mathrm{V_{ref}}$ is the reference (original) displacements. Given that developing torque and volumetric losses models are scaled, particular cases of a polynomial surface fit for unit 1, unit 2 as well as unit 3 can be obtained and shown in **Figure 3.2**.

$$\lambda = \sqrt[3]{\frac{V_{scaled}}{V_{ref}}} \tag{3.15}$$

$$Q_{s,scaled} = f_Q(\Delta p, \omega, \beta)\lambda^2 \tag{3.16}$$

$$T_{s,scaled} = f_T(\Delta p, \omega, \beta)\lambda^3 \tag{3.17}$$

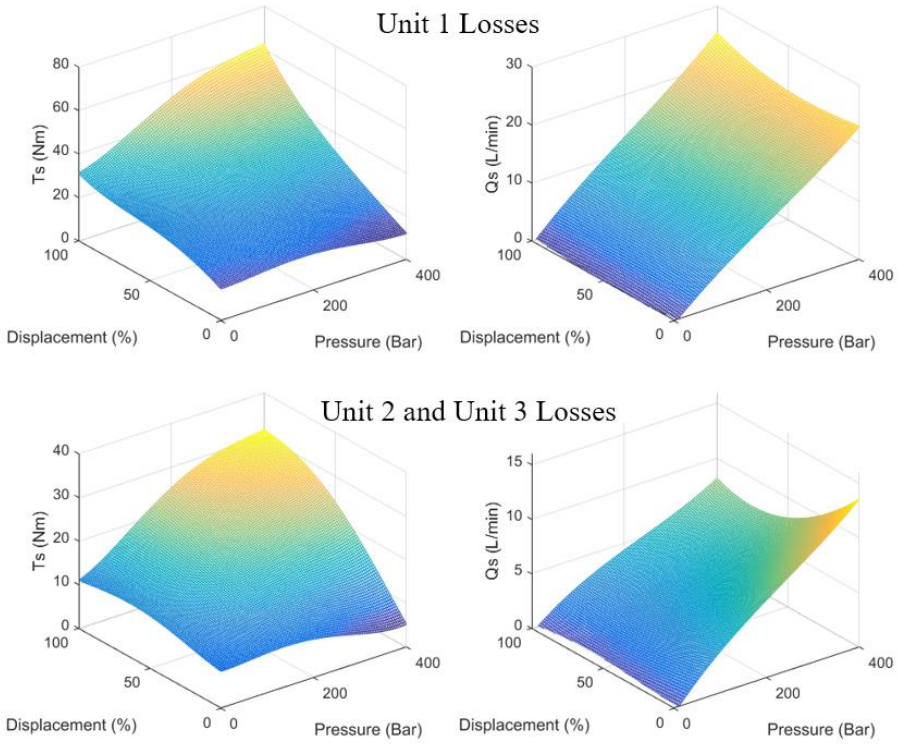

Figure 3.2: Losses for Hydraulic Units

Axial piston machines are talented in operating either as pump or motor with four distinct modes depending on its swashplate position (nominal or over-center), location of high pressure port, and direction of rotation, whose schematic is illustrated by **Figure 3.3**. Therefore, as a result of four-quadrant operations in both pumping and motoring mode, a sign convention figure is given in **Figure 3.4** to clarity various running modes.

On the one hand, effective flow rate and torque can be computed by Equation (3.18) and Equation (3.19) in pumping mode. Where Q_{th} and Q_s is coming from Equation (3.11) and Equation (3.13) separately; T_{th} and T_s are defined in Equation (3.12) and Equation (3.14) respectively.

$$Q_{eff} = Q_{th} - Q_s \tag{3.18}$$

$$T_{eff} = T_{th} + T_s \tag{3.19}$$

On the other hand, Equation (3.20) and Equation (3.21) can definite effective flow rate and torque in motoring mode.

$$Q_{eff} = Q_{th} + Q_s \tag{3.20}$$

$$T_{eff} = T_{th} - T_s \tag{3.21}$$

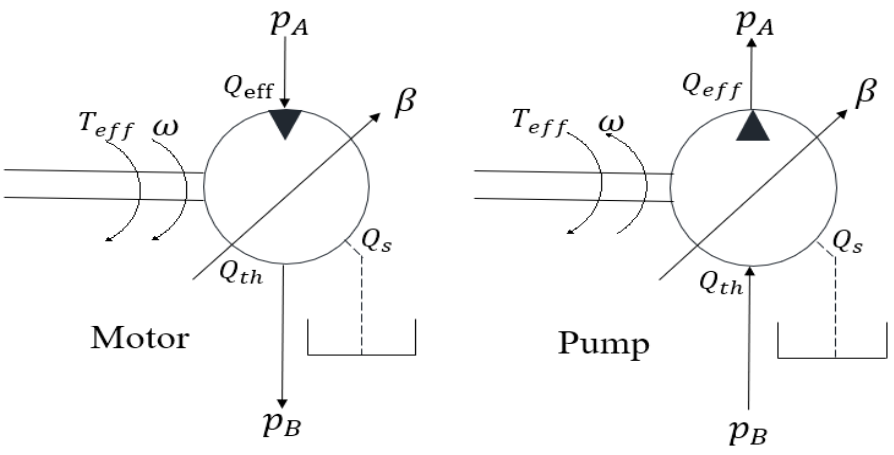

Figure 3.3: Diagram of Motor and Pump

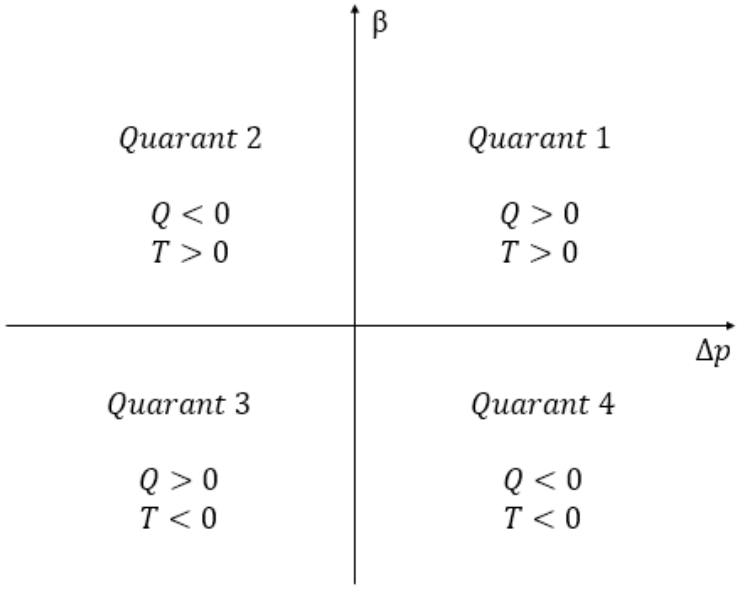

Figure 3.4: Sign Convention for Pump/Motor Four-quadrant Operation

3.2.2 Bladder Accumulator

A bladder type hydro-pneumatic accumulator shown in **Figure 3.5** is applied in both high pressure and low pressure accumulator. It has two possibilities to connect with line either linked with system directly as series hybrids or disconnected with system by enabling valve as blended hybrids. In Maha HHV, the indirect connected method is utilized in both LPA and HPA.

As an energy storage device, HPA is supposed to store the energy achieved by compressing nitrogen gas because of pumping pressurized fluid from the inlet of oil side, and make use of this reversed energy as an auxiliary power for helping engine to propel vehicle in the future. From hydraulic system point of view, accumulator should be regarded as a component providing hydraulic capacitance and hydraulic flow when it is coupled with system. Those equations can be given by Equation (3.22) and Equation (3.23).

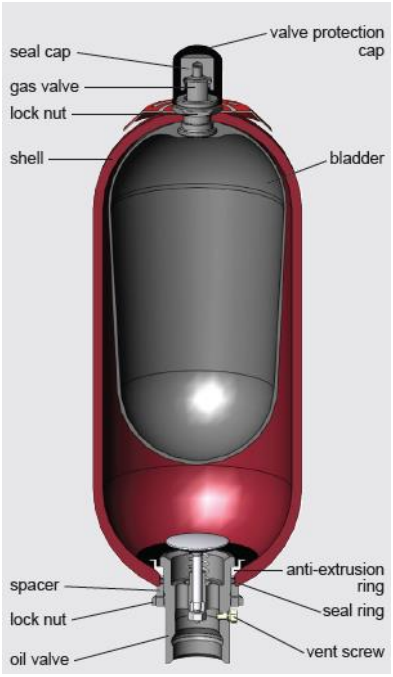

Figure 3.5: Bladder Accumulator [27]

$$\dot{p}_{acm} = \frac{Q_{acm}}{C_{acm}} \tag{3.22}$$

$$C_{acm} = \frac{V_0}{n} \cdot \left(\frac{p_0}{p_{acm}^{n+1}}\right)^{\frac{1}{n}} \tag{3.23}$$

However, from energy storage system point of view, an ideal gas model with polytrophic process should be employed. Since the volume of HPA had been sized by advanced optimum methodology [21], the energy storing capability which is a function about volume, pre-charge pressure and minimum as well as maximum pressure, has already settled. The energy capacity of a hydraulic accumulator for an ideal gas can be defined as Equation (3.24) [28].

$$E_{capacity} = \frac{p_{min} V_0 \left(\frac{p_0}{p_{min}}\right)^{\frac{1}{n}}}{1-n} \cdot \left[1 - \left(\frac{p_{min}}{p_{max}}\right)^{\frac{1-n}{n}}\right] \tag{3.24}$$

where

- $E_{capacity}$ is the energy capacity of the accumulator
- V_0 is the volume of the accumulator
- p_{min} is the minimum pressure
- p_{max} is the maximum pressure
- p_0 is the pre-charge pressure of the accumulator
- n is the adiabatic constant for nitrogen

3.2.3 Check Valves, Relief Valves and Enabling Valve

Check valves and relief valves are derived applying orifice flow equation as their mathematic model. But from functional perspective, they have distinct purposes: check valves allow flow only through one direction while relief valves are defined as a limitation of the maximum pressure in the system. The check valve model is given by Equation (3.25), and that of relief valve is given by Equation (3.26).

$$Q_{check} = \begin{cases} C_v\sqrt{2(p_{in} - p_{out})/\rho}, & p_{in} > p_{\text{out}} \\ 0, & p_{in} \le p_{\text{out}} \end{cases} \tag{3.25}$$

$$Q_{relief} = \begin{cases} C_v\sqrt{2(p_{in} - p_{lim})/\rho}, & p_{in} > p_{\text{lim}} \\ 0, & p_{in} \le p_{\text{lim}} \end{cases} \tag{3.26}$$

where

- $\mathrm{Q_{check}}$ and $\mathrm{Q_{relief}}$ are the flow through a check valve and a relief valve distinctly
- $\mathrm{C_v}$ is the coefficient of flow through valve
- $\mathrm{p_{in}}$ and $\mathrm{p_{out}}$ are the pressure at inlet and outlet of a valve seperately
- ρ is the density of hydraulic fluid
- $\mathrm{p_{lim}}$ is the maximum limitation pressure of a relief valve

Besides, enabling valves with normally closed (N.C.) are able to be considered as manual control switches. Therefore, Boolean function with switching delay can be applied to model it. When it has not received command of open, an open-circuit without any flow passing through is regarded. Once it has switched to another position (open), it must be deemed as a conducting line, and hydraulic flow can go through it freely.

4. Control Algorithm Development

4.1 Electronic Control and Data Acquisition System

For validating and realizing control system, data acquisition system and real-time electronic control system are required. A National Instruments (NI) platform which has a user-programmable micro-processor FPGA as an embedded controller providing high-speed control and custom timing as well as triggering in hardware, six different input/output cards connecting directly to actuators as well as sensors for commanding or gathering information such as pressure, temperature, and speed, is applied to implement the control and data acquisition system, shown in **Table 4.1**. Owing to continuous improvement of Maha HHV, a relay output module named NI-9482 is added in the cause of governing the new enabling valve for low pressure accumulator and the existent enabling valve which is connected to high pressure accumulator.

Table 4.1: Information of National Instruments Platform

Instrument	Specifications
NI cRio – 9074	Real-time controller
NI Module 9205	±10 V, 16 channel analog input
NI Module 9264	±10 V, 32 channel analog output
NI Module 9213	16 channel thermocouples
NI Module 9401	5 V, 8 channel digital input
NI Module 9474	24 V, 8 channel digital output
NI Module 9482	4 channel SPST relay

After hardware implementation, a user interface software from NI called VeriStand helps to get up monitoring system, hardware-in-the-loop and control cells. All control strategies firstly are deployed in MATLAB/SIMULINK environment, and then a co-operation software system with several SIMULINK blocks including data acquisition system and control system is built in VeriStand, which is deployed on cRIO eventually. The embedded controller updated on the cRIO is supposed to read the measurements from various analog and digital input modules, and operate automatically through VeriStand once the control strategies have been developed in SIMULINK successfully.

As a result of NI cRIO hardware collaboration with NI VeriStand software, a system ensured a reliably high-frequency (100 Hz) with capabilities of reading, computing, reacting on inputs in an appropriately short time, is employed to be a real-time electro-mechanical controller as well as data acquisition system.

Since the hardware part has been built up, the next step is engaged to developing suitable control tactics However, throttle pedal and brake pedal are regarded as the only two commanded signals from drivers in the reality. Controller is capable of generating suitable control signals such like the position of enabling valve, displacements of hydraulic units and engine speed to drive vehicle as well as to switch diverse driving modes automatically based

on requirements of driver. A top-level operation scheme including control and data acquisition is displayed in **Figure 4.1**.

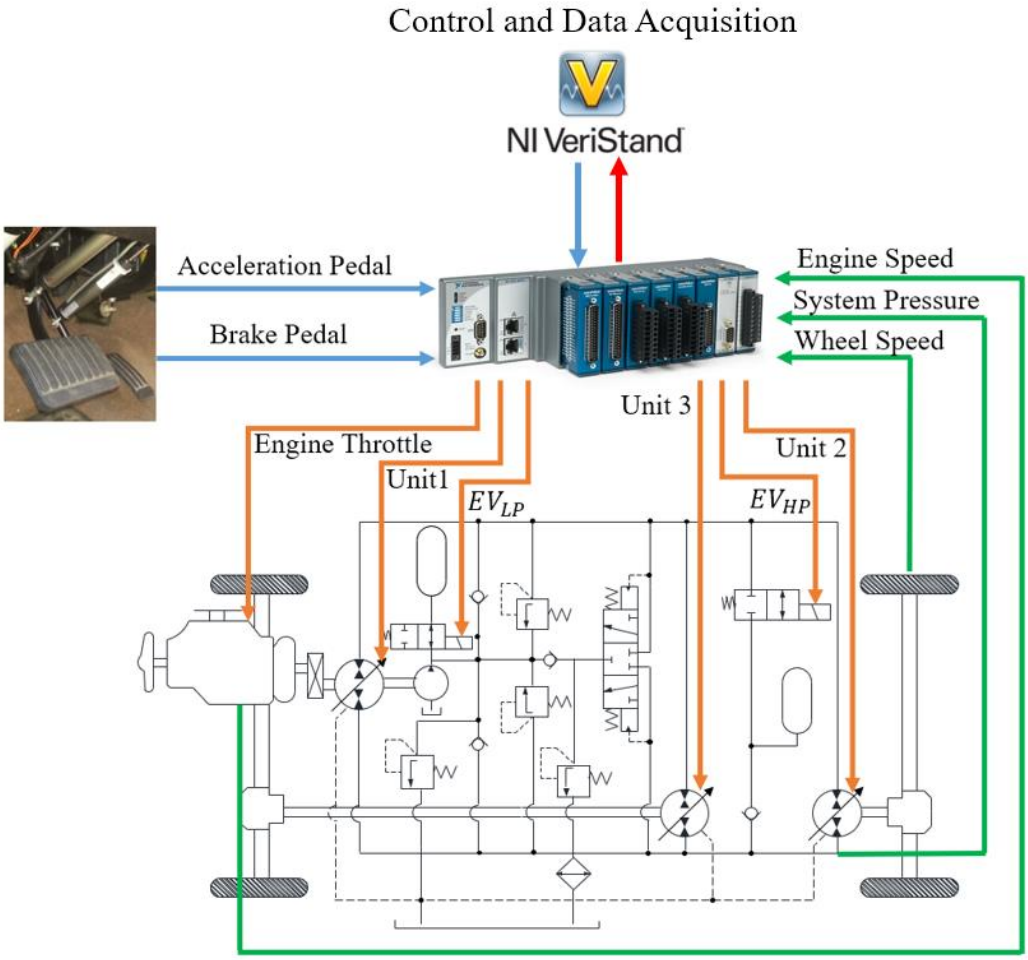

Figure 4.1: Top-level Control Scheme for Maha HHV

4.2 Novel Torque Based Braking Control Strategies

In traditional automotive braking system, brake pedal is mechanically linked to master cylinder. When brake pedal is depressed, the pressure on the brake pedal moves a piston in the master cylinder, forcing the brake fluid from the master cylinder through the brake lines and flexible hoses to the calipers and wheel cylinders. The force applied to the brake pedal produces a proportional force on each of the position. The calipers and wheel cylinders contain pistons which are connected to disc brake pads. Each output piston pushes the attached friction material against the surface of the rotor or wall of the brake drum, thus slowing down the rotation of the wheel. Therefore, brake pedal travel is corresponding to braking force or torque owing to certain material and surface area of brake pads.

However, a new brake system was designed to achieve merely regenerative braking during initial 35% of brake pedal travel, and activate the friction brake by means of actuating master cylinder for aggressive braking under the rest of 65%. In order to realize above-mentioned functionality, the brake pedal mechanism was modified to enable additional pedal travel which was sensed purely electronically and used as a control input for the regenerative braking system

[29]. Under a majority of the working conditions, regenerative braking is able to provide sufficient torque during braking events while friction brake operates as safety brakes just in case, extreme braking actions or hydraulic system cannot generate torque for example. A scheme of modified brake pedals built by CAD and a diagram of the brake pedal position versus brake cylinder pressure are shown in **Figure 4.2**, **Figure 4.3** separately. It can be noticed that master cylinder pressure maintains zero before 35% of brake pedal travel; in other words, friction brake is not activated and regenerative brake works only in this part, which is supposed to recover as much kinetic energy and gravitational potential energy as possible during braking.

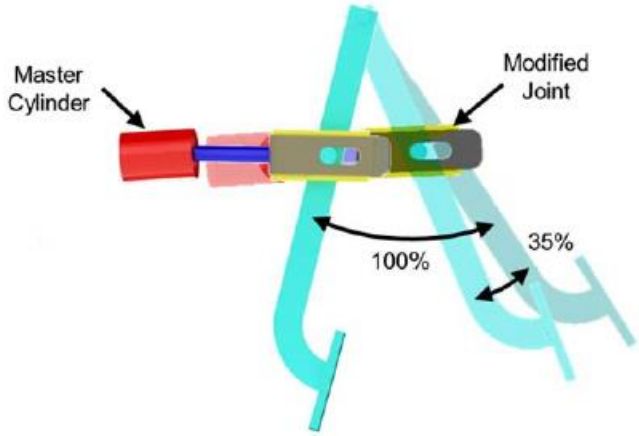

Figure 4.2: Modified Brake Pedal [29]

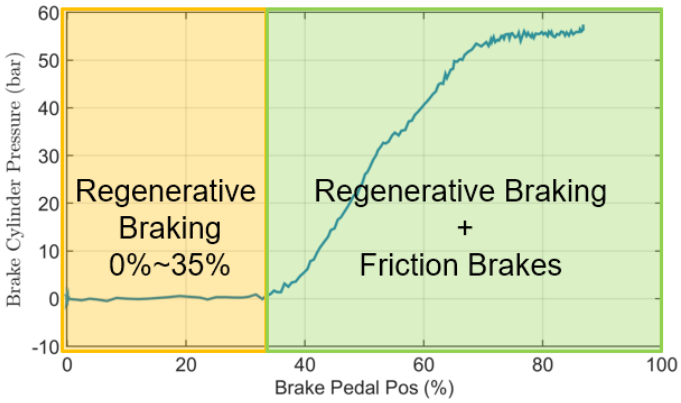

Figure 4.3: Relationship between Brake Pedal Position and Brake Cylinder Pressure

4.2.1 Torque Mapping

As mentioned above, before brake pedal position reaches 35%, only regenerative braking is activated. Once regenerative braking has been in operating mode, unit 2 as well as unit 3 is controlled by pedal position with forcing unit 1 to be zero displacement. Since regenerative braking is a brake by wire system, suitable logics should be established to build the relationship between brake pedal position and the intensity of regenerative braking so that it operates not only much closer to conventional brake system but also collects energy.

However, various kinds of methods such as pressure, deceleration rate have been attempted to develop on regenerative braking, the most logical, appropriate approach is a torque based strategy which aims to control displacements of unit 2 and unit3 to match desired braking

torque corresponding to both brake pedal position and state of charge of high pressure accumulator. This relationship is represented by Equation (4.1). Therefore, a proper lookup table of torque mapping becomes a critical part of design regenerative brake for improving braking performance as well as enhancing driving comfort.

$$T_{23,brake} = T_{brake,map}(u_{brake\ pedal}, p_{HPA}) \tag{4.1}$$

Firstly, maximum braking torque which is derived from hydraulic system should be calculated. There are two particular points: minimum SOC of high pressure accumulator with maximum displacements and maximum SOC of high pressure accumulator with maximum displacements respectively. According to Equation (3.12), the former is the maximum torque under the lowest point of SOC of HPA condition with 244 Nm, the latter is the maximum torque under the highest point of SOC of HPA condition with 810 Nm, whose efficiency is considered as 0.85 totally.

Secondly, for the purpose of keeping almost the same driving feel as conventional vehicle during braking, a baseline test shown in **Figure 4.4**, which was measured when range rover was not served as a platform of the blended hybrid, and a one-dimensional vehicle model shown in **Figure 3.1** with some assumptions including vehicle running in horizontal roads with concrete road and neglecting inertial dissipation of shaft, are employed to find out the interpolation of braking torque related to brake pedal position. The equation applied to compute required torque is given by Equation (4.2).

$$T_b = \left(m\frac{dv}{dt} - F_a - F_g - F_r\right) \cdot r_{wheel} \tag{4.2}$$

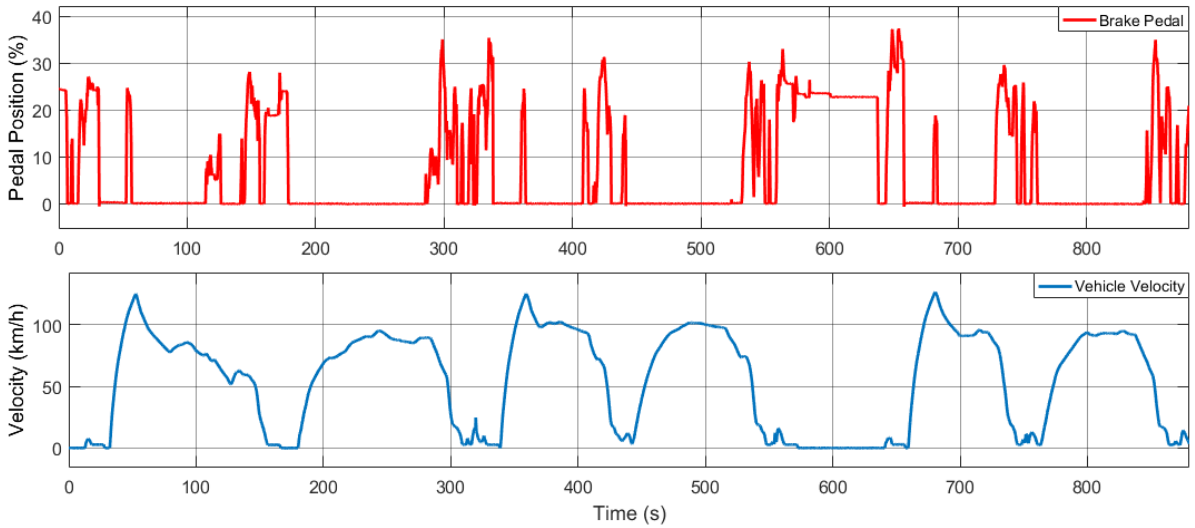

Figure 4.4: Original Baseline Test

Finally, given that deceleration rates proposed or observed by most of the researchers are less or equal to deceleration rate proposed by Institution of Transportation Engineers in 1999, and by American Association of State Highway and Transportation Officials (AASHTO) in 2004, comfortable deceleration rate should not be larger than 3.4 m/s^2 [30]. An adjusted lookup table applicable for Maha HHV had been found out shown in **Figure 4.5**. This lookup table

guarantees that braking torque corresponding to brake pedal position is almost the same as original, and deceleration rate is not over 3.4 m/s^2 under 35% of brake pedal travel.

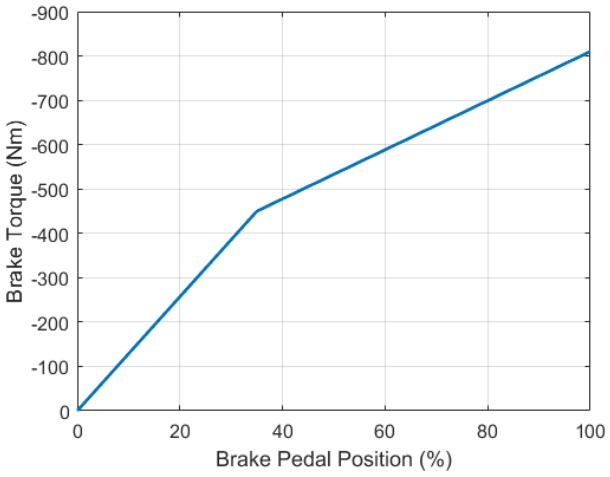

Figure 4.5: Torque Mapping for Regenerative Braking

4.2.2 Feedback Control

A feedback control system whereby the signal to be controlled is compared to a desired reference signal and the discrepancy used to compute corrective control action, is able to deal with uncertainty to a certain extent [32] [33]. Therefore, a feedback control system with a proportional–integral–derivative (PID) controller expressed mathematically as Equation (4.3), was designed for regenerative braking, whose block diagram is shown in **Figure 4.6**.

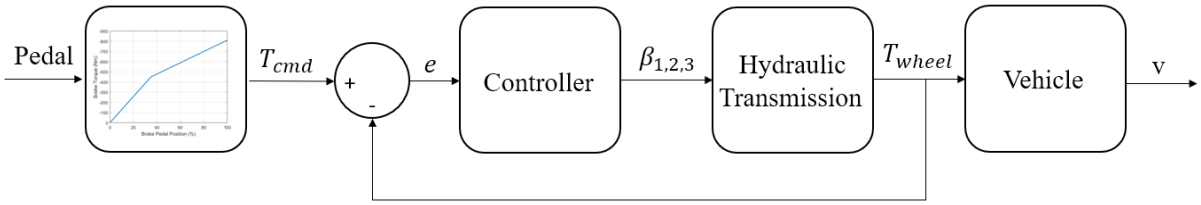

Figure 4.6: Feedback Control Diagram

$$u(t) = K_p e(t) + K_i \int_0^t e(\tau)d\tau + K_d \frac{e(t)}{dt} \tag{4.3}$$

In the cause of tuning the parameters inside PID controller accurately, state-space equations whose common form is given by Equation (4.4) and Equation (4.5) where A is the state (or system) matrix, B is the input matrix, C is the output matrix and D is the feedforward (or feedthrough) matrix, were found out with the help of LMI Control Toolbox [34] in MATLAB. They represent system plant including actuators (hydraulic units) and system (hydraulic transmission line). For the regenerative braking, this is a single-input-single-output (SISO) system; the state (x) and input (u) vectors are in Equation (4.6) and Equation (4.7) separately.

$$\dot{x} = Ax + Bu \tag{4.4}$$

$$y = Cx + Du \tag{4.5}$$

$$x(t) = (p_A \;\; p_B \;\; p_{HPA} \;\; \omega_{wheel})^T \tag{4.6}$$

$$u(t) = (\beta_1 \;\; \beta_2 \;\; \beta_3)^T \tag{4.7}$$

Control System Toolbox in MATLAB enables user to analyze, design, and tune parameters of controller by interactive techniques such as Bode diagram in frequency-domain and step respond in time-domain. The PID controller was tuned by using Control System Toolbox in MATLAB with known state-space equations. The close-loop system with suitable tuning PID controller is demonstrated by **Figure 4.7**. The blue line represents the open-loop characteristic; the red line represents characteristic of sensitivity function which tells the relationship between reference signal and tracking error; and the orange line represents characteristic of complementary sensitivity function which tells the relationship between tracking error and output signal. It can be noticed that open-loop system has a high gain in low frequency part to guarantee a fast respond in close-loop system whereas closed loop system has a unitary loop-gain, and the attenuation reaches -3dB at 100 rad/s.

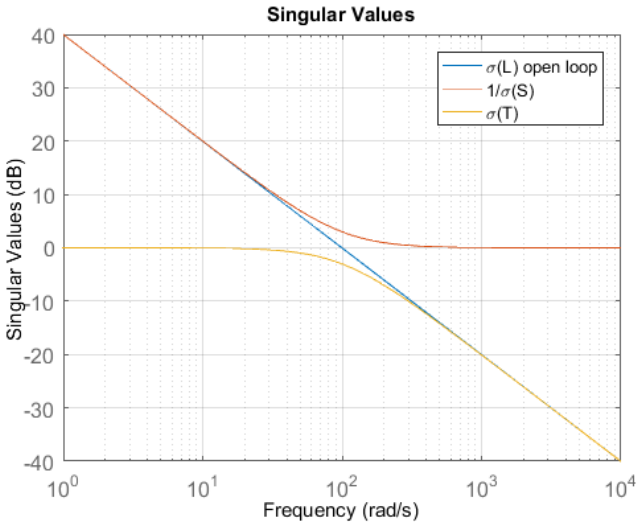

Figure 4.7: Frequency-domain Analysis

Time-domain analysis was contributed by running entire system in simulation to verify not only performance of controller but also the pre-define lookup table which is one-to-one correspondence between brake pedal position and required torque mentioned in **Figure 4.5**. A partial original baseline drive cycle would be in use to validate this torque based controller. The testing method was to accelerate vehicle reaching the same velocity of the baseline drive cycle, and then, brake pedal position served as the only input signal to command brake controller to monitor displacements of unit 2 and unit 3 under circumstances with diverse SOC of HPA and pump speed variation on behalf of verifying whether hydraulic system was able to meet the required torque or not.

Simulation result is demonstrated from **Figure 4.9** to **Figure 4.12** and the brake pedal inputs are shown in **Figure 4.8**. According to **Figure 4.9** and **Figure 4.12**, during braking events, modified system was almost completely matching original system both on vehicle velocity and

braking torque no matter how SOC of HPA and speed of unit 2 as well as unit 3 were altered. **Figure 4.10** shows that controller performed quite well in commanding displacements to meet the torque requirements related to input signals. The lower SOC of HPA or lower speed of pump it has, the higher displacements will be. In **Figure 4.11**, since nearly all the fluid flows coming out from unit 2 and unit 3 were going to pressurized line B, line B reached the pressure of HPA at short time under high speed condition; when the pressure was over the pressure of HPA, energy was saved; otherwise, there was no flow through check valve to the accumulator; beyond that, line A maintained constant pressure during braking. Hence, both desirable pre-define lookup table and eligible control method were satisfied design requirements so that same brake pedal travel had an effort on same braking results.

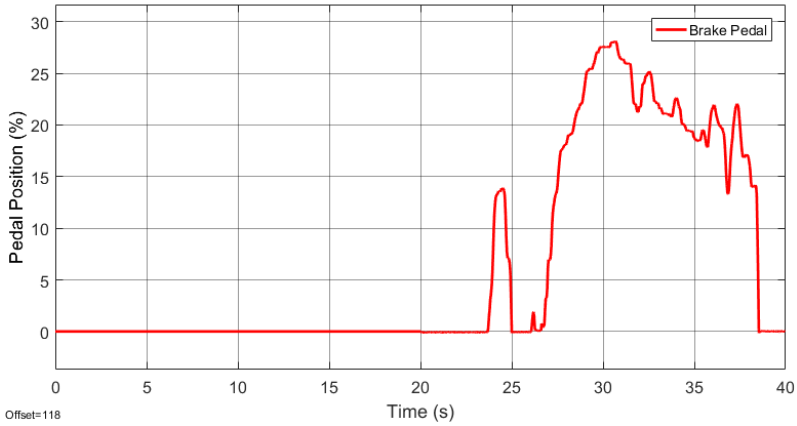

Figure 4.8: Feedback Controller Simulation Result (Brake Pedal)

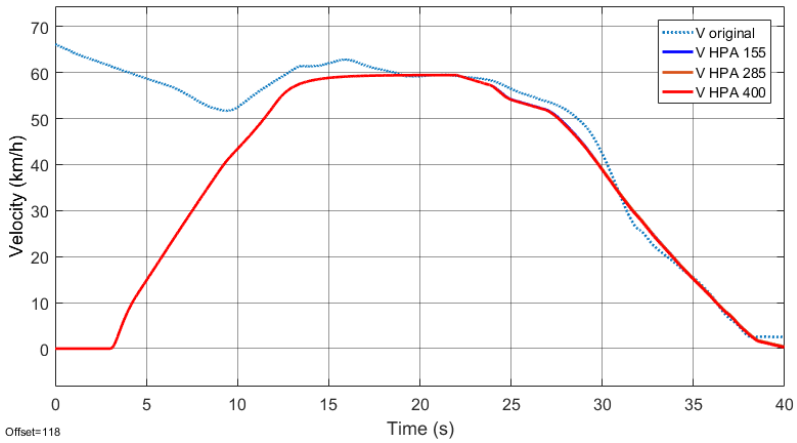

Figure 4.9: Feedback Controller Simulation Result (Vehicle Velocity)

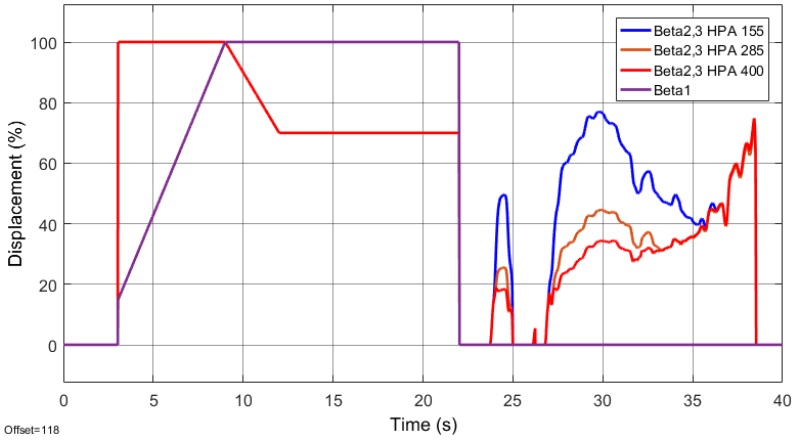

Figure 4.10: Feedback Controller Simulation Result (Displacements of Hydraulic Units)

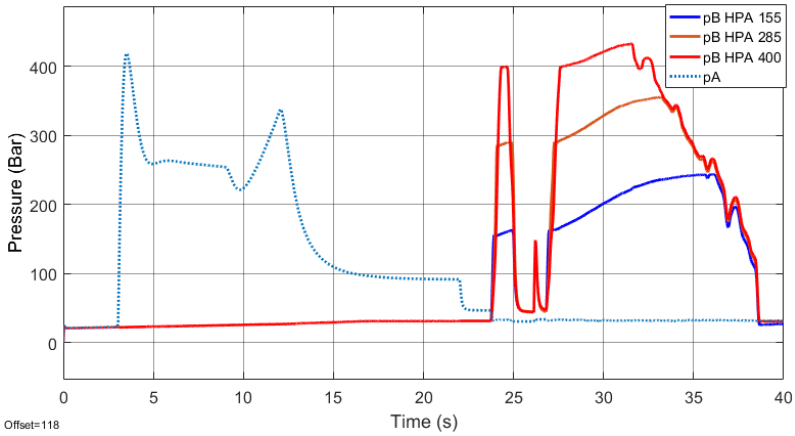

Figure 4.11: Feedback Controller Simulation Result (Line Pressure)

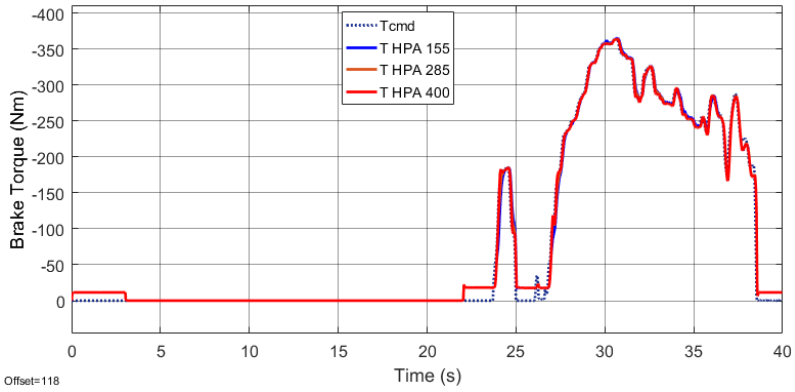

Figure 4.12: Feedback Controller Simulation Result (Torque)

Even though a feedback control system is generally considered superior to an open-loop system, a kind of disadvantages can be expected when feedback control loop is applied: extra charges due to increased number of components such as error detectors and sensor, who are necessary in order to compare two different states; time of remaking hardware to meet the requirement of feedback system. Moreover, driver is capable to handle and compensate the

slight error derived from model uncertainty in the actual braking system. Consequently, a driver closed loop based feedforward control system is introduced and selected to implement in Maha HHV.

4.2.3 Feedforward Control

Since pre-define lookup table has been proved that it is proper for Maha HHV, the main task of feedforward controller is to calculate displacements of unit 2 and unit 3 according to torque command as well as dynamic paraments such as pressure, and to compensate losses as far as possible. Equation (4.8) manifests the computing method of displacements inside controller, where T_{cmd} is torque command derived from brake pedal position mapping on pre-define lookup table; T_s is torque losses donated by above-mentioned losses model and Equation (3.17); V_2 and V_3 are theoretical displacement volume of hydraulic units; p_{HP} is the pressure of high pressure line and yet p_{LP} is that of low pressure line.

Figure 4.13 illustrates the entire feedforward control loop for renarrative braking. Driver is being a commander as well as feedback sensor in the whole system. Apart from without the torque feedback loop inside software level, the rest parts of this control architecture are similar with feedback control logic. Controller is able to monitor parameters including pressure in the line as well as state of charge of accumulator from pressure sensor, and then gives real-time feedback on variation of displacements. Given that computation based on micro-processer is fast enough, from the perspective of electronic control system, it is without delay when feedforward control method is in application; index such as rise time and settling time will not be considered. However, human reaction time and response delay of mechanical components still exist.

$$\beta_{2,3} = \frac{(T_{cmd} + T_s)2\pi}{(V_2 + V_3)(p_{HP} - p_{LP})} \tag{4.8}$$

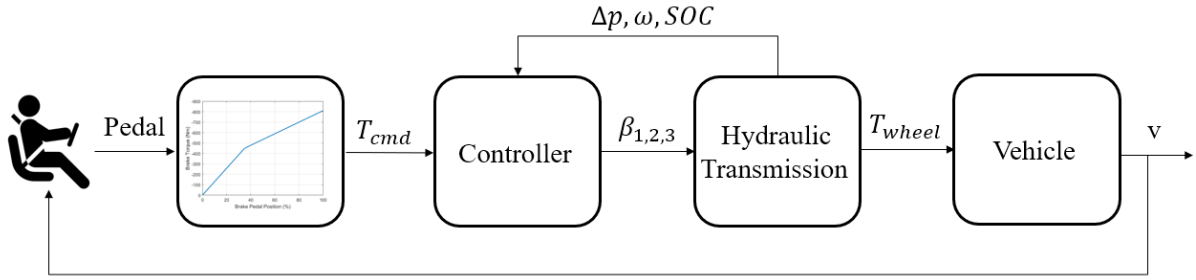

Figure 4.13: Feedforward Control Diagram with Driver-close-loop

On account of having an instant that p_{HP} is equal to p_{LP} when line A transfers from high pressure line to low pressure line and line B transfers to high pressure line by contract, the pressure difference value in the denominator in Equation (4.8) is likely to be zero, which is not permitted. A transitive strategy making use of the differential pressure between high pressure accumulator and the outlet part of low pressure accumulator is to replace aforesaid pressure difference in Equation (4.8). During transition (high pressure line is interchanged between line A and line B), the transitive strategy is applied to control units 2 and 3; since the pressure difference in transitive strategy is not the real differential pressure between inlets and outlets

of hydraulic units, after transition, displacements of unit 2 and unit 3 are still computed by Equation (4.8).

In order to obtain knowledge about human control behavior and validate controller with stander drive cycle such as Urban Dynamometer Driving Schedule (UDDS), a longitudinal dynamics controller based on PID was applied to be the driver model. The controller compensates for errors between the desired and actual acceleration or deceleration [35]. If the simulation velocity derived from vehicle model is smaller than presupposed velocity in braking condition for example, the controller will command deeper brake pedal position on behalf of following the desired velocity profile. In the meantime, deeper brake pedal position induces higher braking torque which is controlled by brake control system, thus simulated velocity is supposed to meet desired velocity. The total simulation block diagram with driver model is shown in **Figure 4.14**.

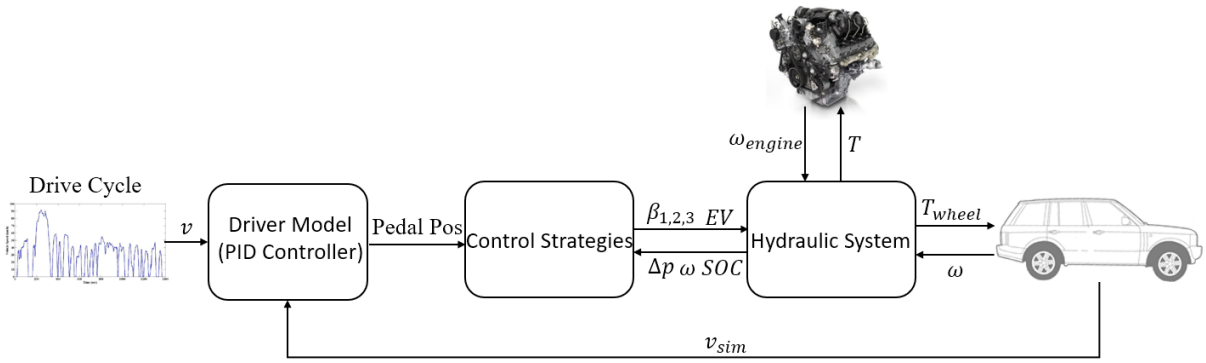

Figure 4.14: Simulation Block Diagram with Driver Model

Since hybrid driving mode had effort on state of charge of high pressure accumulator in acceleration, non-hybrid driving mode was devoted to running feed-forward controller validating simulation in a simple UDDS drive cycle. This test had three different initial condition of HPA, 155 bar, 285 bar and 400 bar respectively. Further, driver model took part in for a closed loop vehicle-driver simulation; hence, pedal position could be regarded as descriptions of driver behavior. **Figure 4.15** illustrates the brake pedal position in different SOC of HPA, but different initial state of HPA had limited impact on driver behavior during braking.

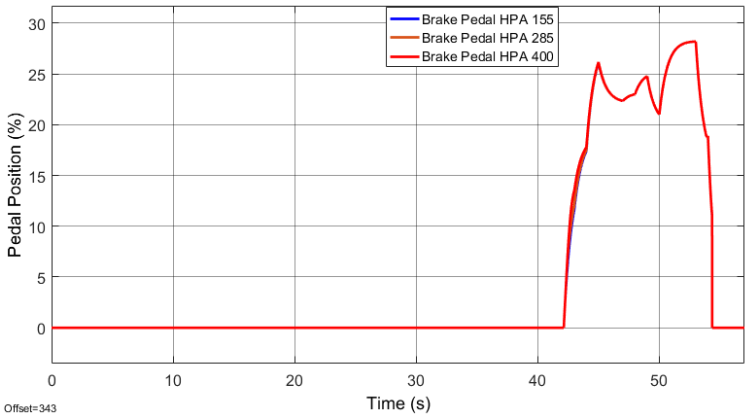

Figure 4.15: Feedforward Controller Simulation Result (Brake Pedal)

The same conclusion can be obtained by analyzing vehicle velocity in **Figure 4.16**: even though driver model existed a certain degree of reaction delay, three driving simulations had similar results matching the profile of UDDS drive cycle. Therefore, braking performance and drivability depend on brake pedal travel derived from driver. The diversities are reflected on displacements, shown in **Figure 4.17**. Displacements of units 2 and 3 were changed to match command torque and unit 1 maintained zero displacement, while energy was recovered by charging high pressure accumulator with increasing pressure in line B indicated by **Figure 4.18**.

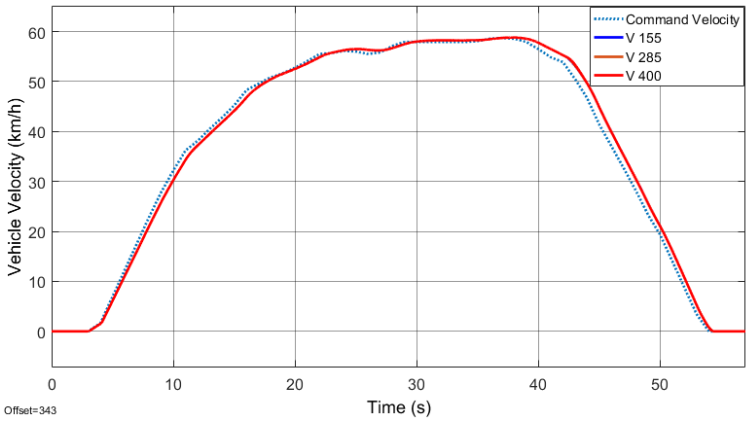

Figure 4.16: Feedforward Controller Simulation Result (Vehicle Velocity)

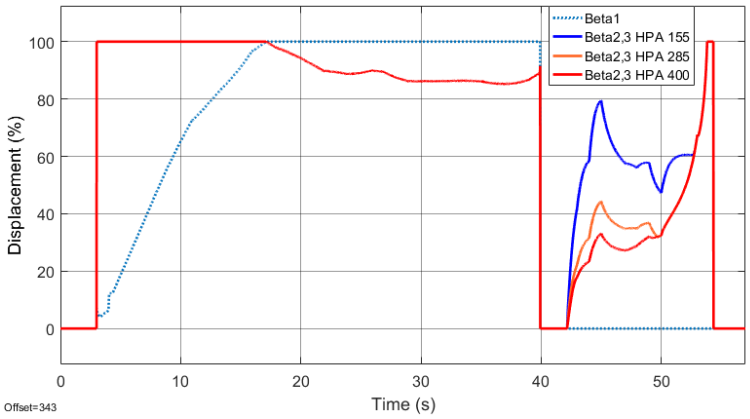

Figure 4.17: Feedforward Controller Simulation Result (Displacements of Hydraulic Units)

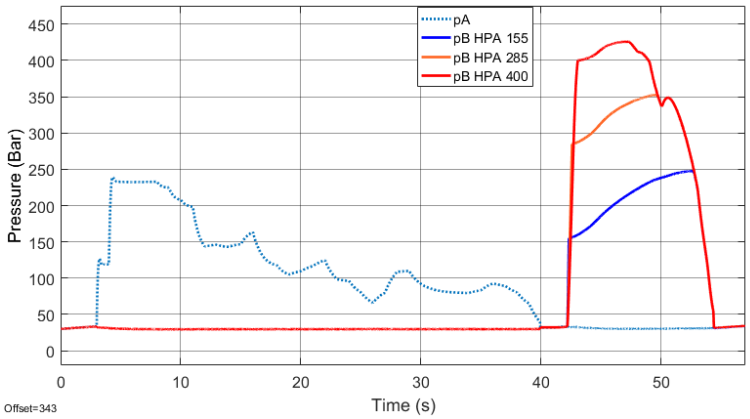

Figure 4.18: Feedforward Controller Simulation Result (Line Pressure)

Figure 4.19 demonstrates that system torque was able to coincident with command torque as far as possible because torque losses due to pressure, speed and displacement had been considered inside feedforward controller when it was designed. Eventually, as one of the concerned index of driving comfort, deceleration rate is around 1.4 m/s^2 as shown in **Figure 4.20**, which is far below uncomfortable threshold valve on the premise of guaranteeing braking performance.

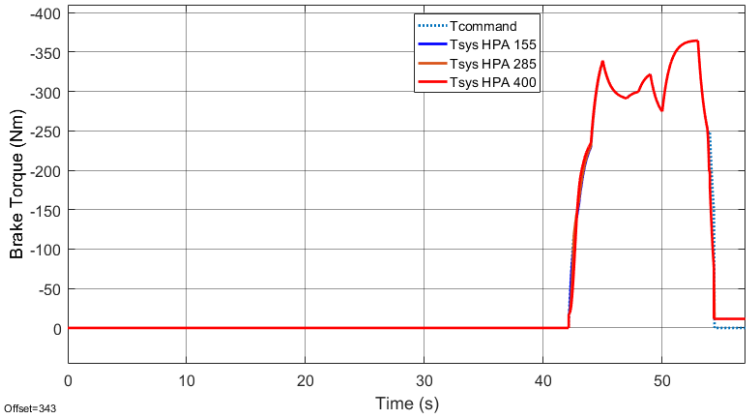

Figure 4.19: Feedforward Controller Simulation Result (Torque)

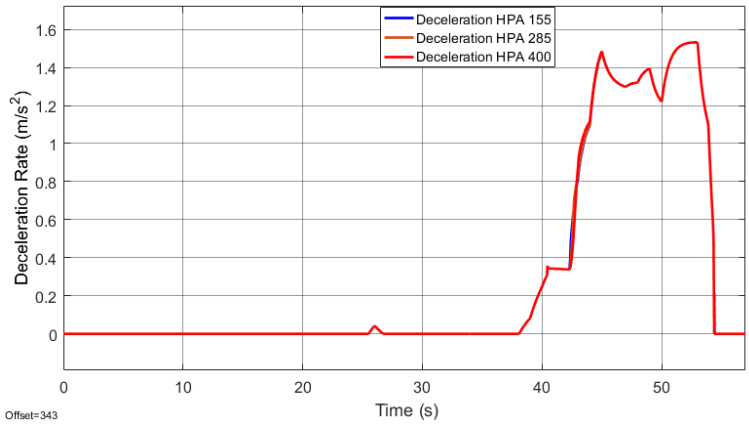

Figure 4.20: Feedforward Controller Simulation Result (Deceleration Rate)

From what has been discussed above, it is torque based control that brake system has already applied, the outline of brake torque and deceleration rate are proportional to pedal position while displacements of hydraulic units are changed with torque requirement as well as pressure. As a result, torque based regenerative braking system has better drivability and performance than that of previous control method which was introduced by Tyler J. Bleazard as well as Hiral Haria [21][22]. Furthermore, it is much closer to conventional automobile.

4.3 Supervisory Control

Although desirable regenerative brake controller had been studied and validated, the issue that accumulator will be likely to be fully charged if it is not in used frequently under urban driving circumstances or it is charging during long braking with downhill condition is inescapable.

When HPA is full and regenerative braking keeps working, extra fluid flow that should have stored in HPA is conscripted to pass through high pressure relief valve accompanied with heat. With the increase of temperature, not only system efficiency will decrease, but also do harm to hydraulic units. There are two approaches for resolving aforesaid issues.

4.3.1 Supervisory Control for Brake

On the one hand, building up a supervisory control illustrated in **Figure 4.21**, for preventing regenerative braking from working on full-charge of accumulator that may be induced by long braking condition, is an effective solution. When pressure of HPA is detected over pre-set valve 430 bar in this case, all displacements of hydraulic units are forced to be zero, which means regenerative braking is disable. At the same time, friction braking has to be activated to make up for braking torque that should have provided by regenerative braking.

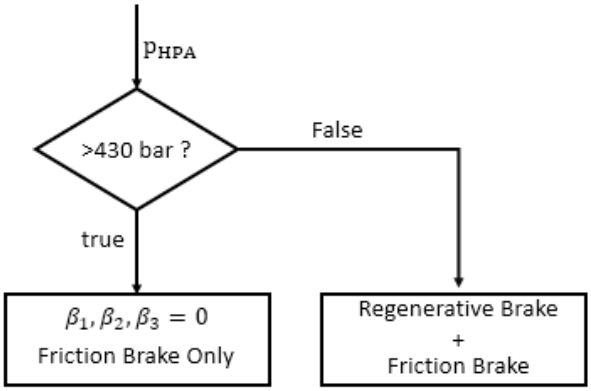

Figure 4.21: Supervisory Control Logic for Brake

4.3.2 Supervisory Control for Acceleration

On the other hand, another methodology is to utilize accumulator as much as possible. Several criteria are shown in **Figure 4.22** including pressure of HPA should be larger than its pre-charge pressure as well as line A pressure; command torque is not lower than system torque; vehicle velocity should be greater than special valve. Not only are criteria for switching non-hybrid driving mode to hybrid driving mode or vice versa, but also for avoiding charging HPA in acceleration mode. This supervisory controller monitors parameters including pressure of HPA, pressure in the line A, command torque, system torque, vehicle velocity as well all the time. Among them, neither command torque nor system torque are derived from measurements. For command torque, it is generated by acceleration pedal position with torque mapping, which is similar with the relationship between brake pedal position and braking torque. For system torque, it is roughly calculated by inverse vehicle dynamic given by Equation (4.9), where J is inertial moment of vehicle. When and only when all conditions are met, system shifts in hybrid driving mode with opening HPA enabling valve as well as activating secondary control. Otherwise, as long as one of the criteria is not satisfied, vehicle keeps working on non-hybrid mode or shifts from hybrid drive to non-hybrid drive.

$$T_{sys} = \frac{J\dot{\omega}_{wheel} - F_d r_{wheel} - F_a r_{wheel} - F_g r_{wheel}}{i_{axle}\eta_{axle}} - \mathrm{T_{s,scaled}} \tag{4.9}$$

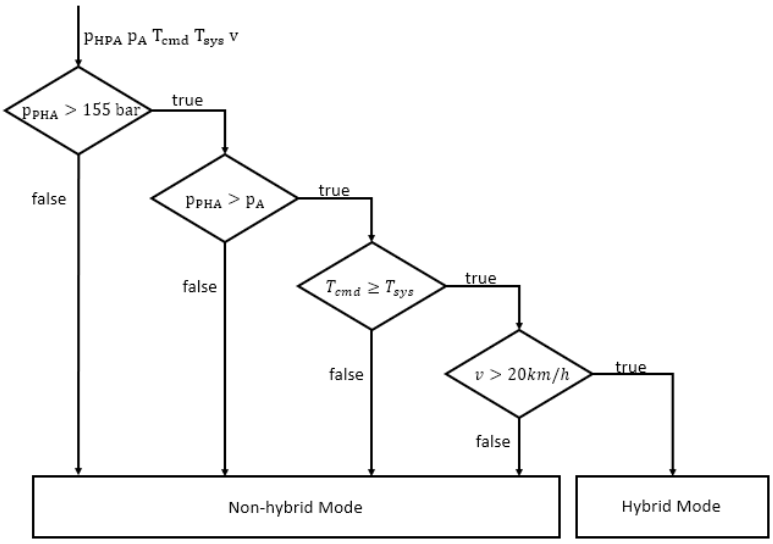

Figure 4.22: Mode Switching Criteria

4.4 Simulation Result

It is available to image that if system always works on non-hydraulic driving mode, after several braking events, accumulator will be highly likely to get full-charge. Once the pressure of HPA is over 430 bar, braking system will be under its supervisory control. For easily reaching threshold valve, initial state of charge in this simulation would be 380 bar. Its simulation results are shown from **Figure 4.23** to **Figure 4.27**. Before pressure of HPA was above 430 bar, regenerative brake served normally in first braking event and a part of second braking event. Once brake supervisory control detected pressure in line B was higher than 430 bar, regenerative brake had to be disactivated. Driver would hit brake pedal harder to attain his desired braking effect indicated in **Figure 4.23**. Although system needed time to switched from regenerative brake to friction brake, simulation velocity matched drive cycle shape as before.

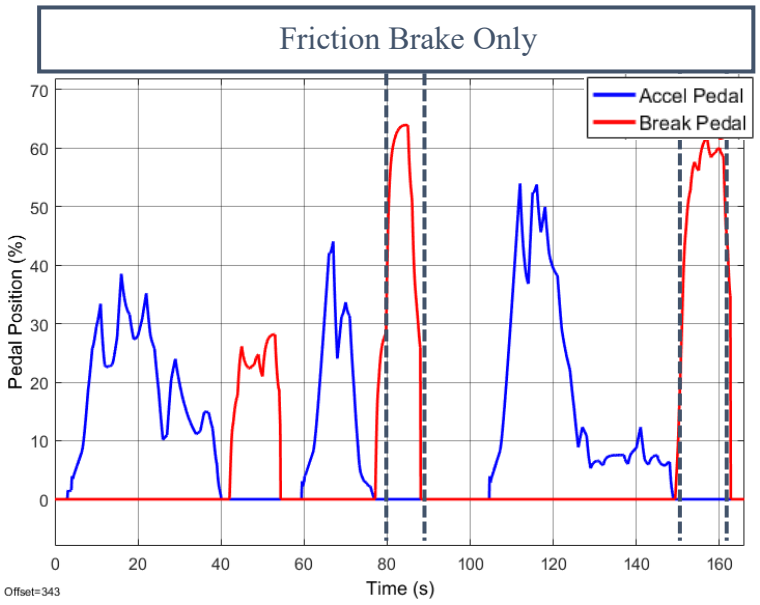

Figure 4.23: Brake Supervisory Control Simulation (Pedal Position)

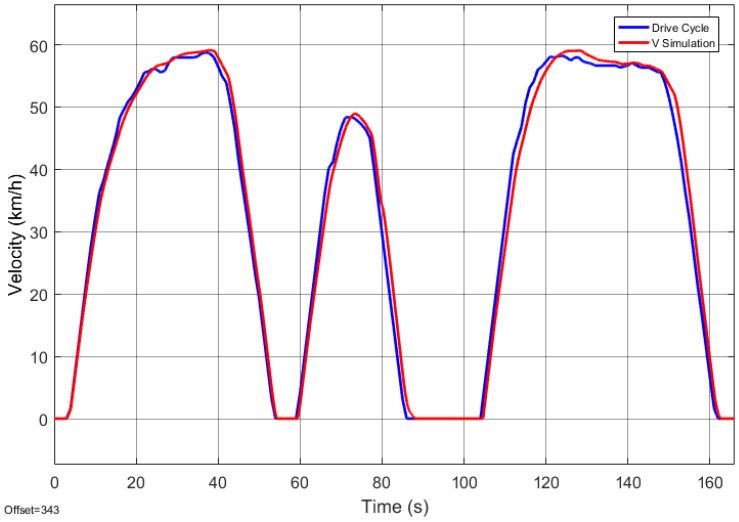

Figure 4.24: Brake Supervisory Control Simulation (Velocity)

It is noticeable that even though requirement of brake torque corresponding to brake pedal position was still the command signal to brake controller seen in **Figure 4.27**, because of patriation of supervisory control to force hydraulic units into zero displacements shown in **Figure 4.25**, and without differential pressure between inlet and outlet of units exposed by **Figure 4.26**, system would not provide brake torque any more.

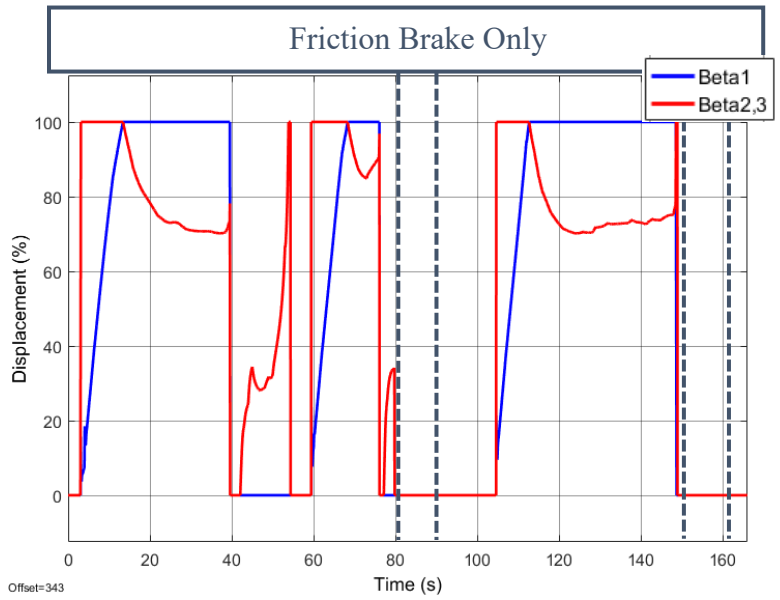

Figure 4.25: Brake Supervisory Control Simulation (Displacement)

Besides, hydraulic transmission severed as much similar to coasting mode when friction brake was in operation only. Pressure in line A as well as line B was equal to the pressure of low pressure accumulator. Since research emphasizes on braking condition, torque of acceleration part was not given in **Figure 4.27**.

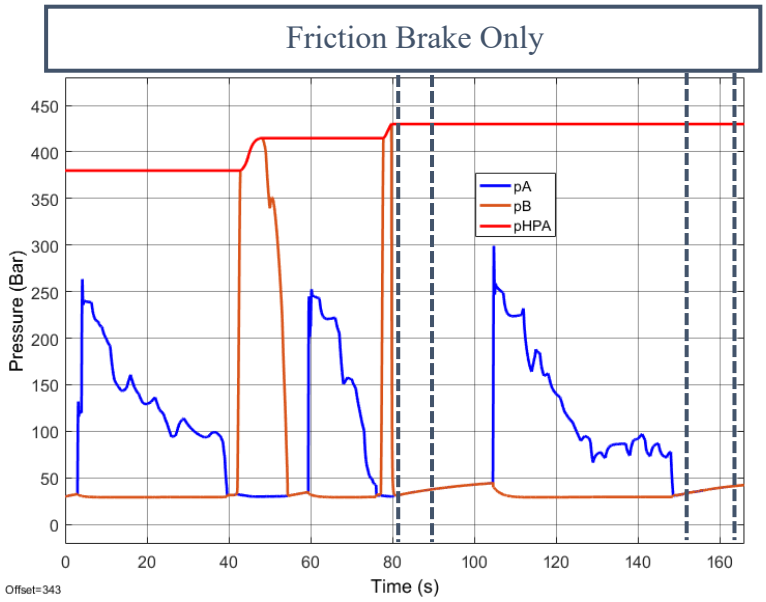

Figure 4.26: Brake Supervisory Control Simulation (Pressure)

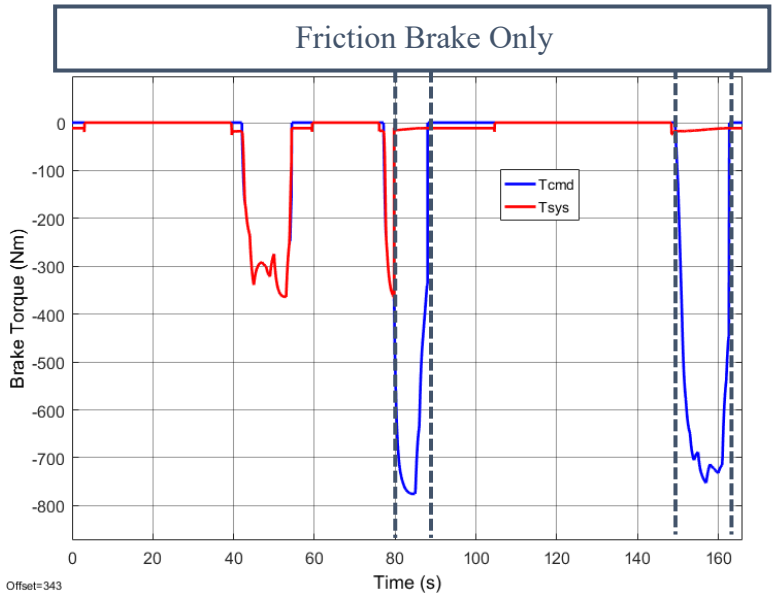

Figure 4.27: Brake Supervisory Control Simulation (Torque)

However, above-mentioned simulation results just reflect system behavior in extremely cases that accumulator is not in use or over charge. As a matter of fact, accumulator is able to be utilized frequently in general driving condition when all criteria of mode-switching are satisfied; therefore, regularly charging and discharging will be its normalcy. Next, UDDS cycle is employed to simulate the situation when vehicle runs in urban areas with regularly stop-and-go pattern. During this simulation, system operates on either non-hybrid mode or hybrid mode automatically.

UDDS drive cycle seen in **Figure 4.28** was the merely input in this simulation. Pedal position indicated the driver's reflection as well as input signal for controller in **Figure 4.29**. According to acceleration or brake pedal position, controller including acceleration, brake as well as supervisory control strategies would generate suitable command signal such as displacements

shown in **Figure 4.30**, enabling valve position to manage power of powertrain to drive vehicle. The same initial SOC of HPA with 380 bar as previous one was used. Nevertheless, hybrid driving mode kept using energy stored in HPA, pressure of HPA was not over 300 bar and not meant to be 430 bar during whole UDDS cycle shown in **Figure 4.31**. When transmission works on hybrid mode, HPA was discharging; when vehicle was braking, energy was stored by charging HPA. **Figure 4.32** indicated that provided torque in the system always matched command torque from driver in simulation. Furthermore, maximum decertation rate exposed in **Figure 4.33** was about 1.5m/s^2 which was quite moderate compared with 3.4m/s^2 in aggressive condition. Total braking torque was derived from regenerative brake controlled by torque based feedforward controller, which means that except reasonable losses, almost all kinetic energy was available to be recovered.

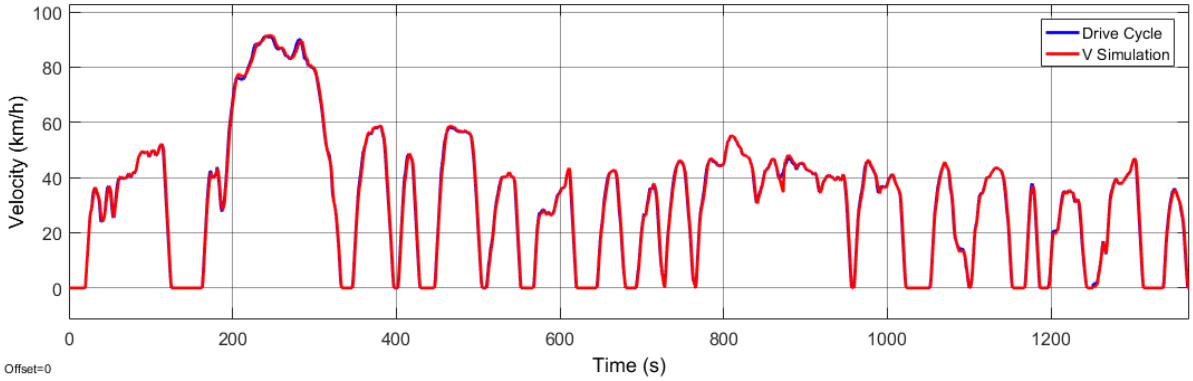

Figure 4.28: Simulation Result with UDDS (Velocity)

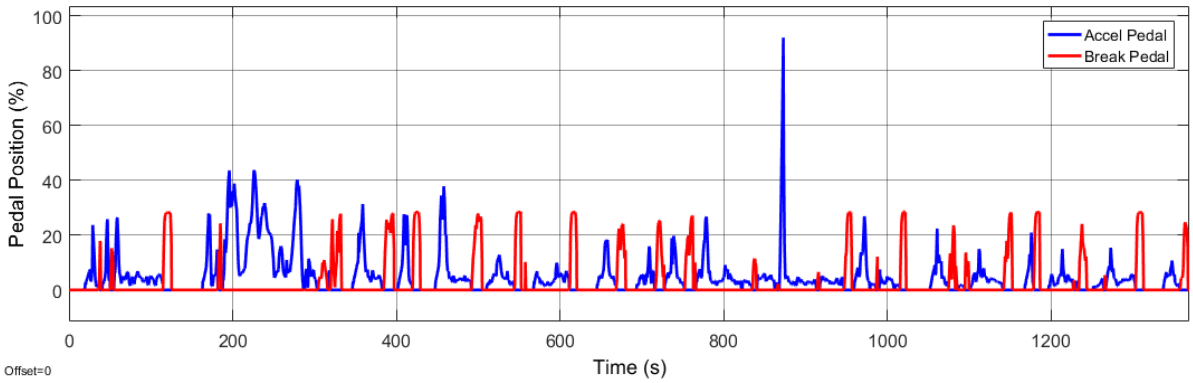

Figure 4.29: Simulation Result with UDDS (Pedal Position)

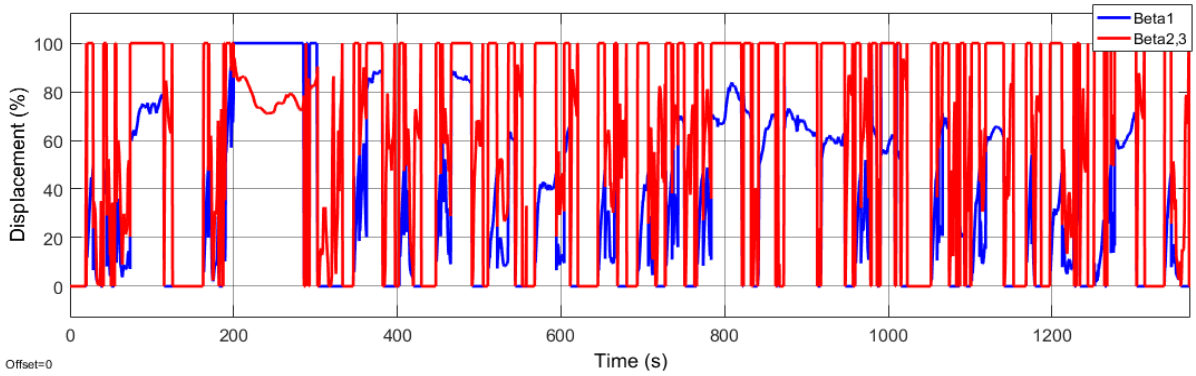

Figure 4.30: Simulation Result with UDDS (Displacement)

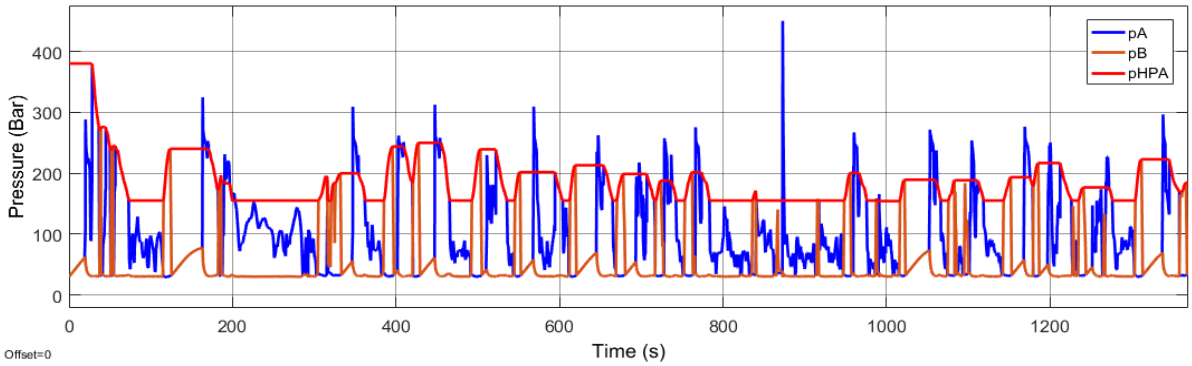

Figure 4.31: Simulation Result with UDDS (Pressure)

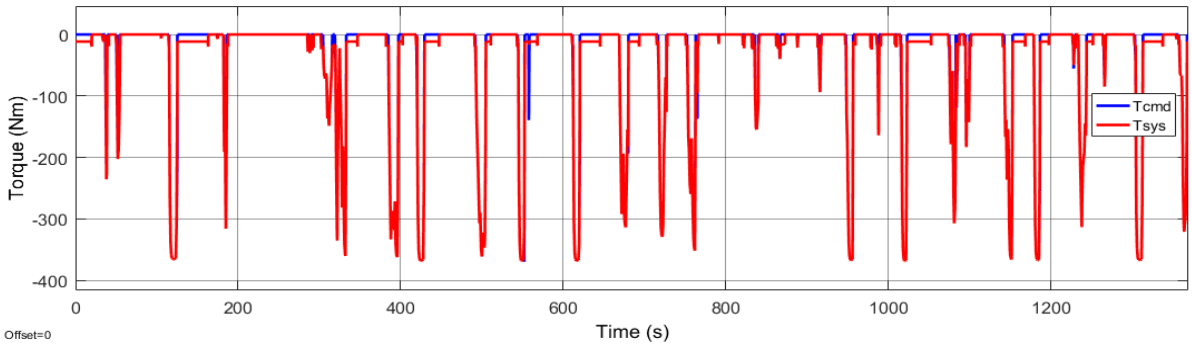

Figure 4.32: Simulation Result with UDDS (Brake Torque)

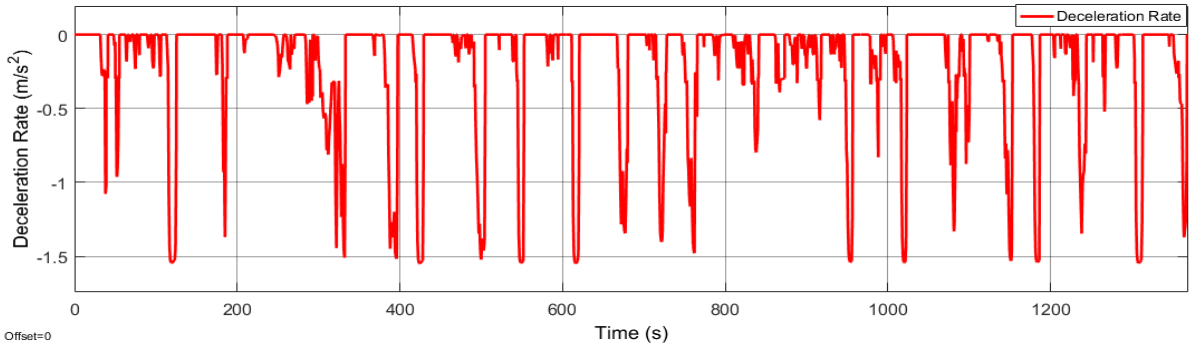

Figure 4.33: Simulation Result with UDDS (Deceleration Rate)

For knowing how much energy that regenerative brake is capable to save, rate of energy recovery exposed by Equation (4.10) comes up, which is defined as the energy saving in hydraulic accumulator given by Equation (4.11) divided by dissipated energy during braking given by Equation (4.12), where ε, E_{HPA} and E_D are the recovery rate, energy collected by accumulator, dissipated energy individually. Δt is braking period, p_i is the instant pressure of accumulator, Q_i is the instant flow into accumulator. Initial velocity and final velocity are represented by v_i and v_f respectively. In this case, potential energy of the gravitational field is zero due to without differential height.

$$\varepsilon = \frac{E_{HPA}}{E_D} \tag{4.10}$$

$$E_{HPA} = -\sum_{i=0}^{\Delta t} p_i Q_i \Delta t \tag{4.11}$$

$$E_D = \frac{1}{2} m\left(v_i^2 - v_f^2\right) - mg(h_f - h_i) \tag{4.12}$$

In order to estimate relatively true rate, an average result computed by each recovery energy rate of ten diverse brake events which are selected from UDDS cycle between 100 second and 725 second, is eligible. Their consequences are shown in **Table 4.2**. From hydraulic system point of view, low pressure with high displacement could have decent efficiency; from vehicle dynamic point of view, the faster velocity it has, the larger drag force will be. Therefore, the lowest recovery rate with 38.62% was reflected in the third brake event due to vehicle speed was up to 90 km/h; the highest recovery rate over 70% appeared on the eighth brake event thanks to high displacement with low system pressure as well as relatively low vehicle speed. Overall, conversion efficiency of regenerative braking is above 60%.

Table 4.2: Energy Recovery Rate

No.	E_{HPA} (J)	E_D (J)	ε (%)
1	1.84×10^5	2.82×10^5	65.25%
2	0.55×10^5	0.93×10^5	59.14%
3	2.02×10^5	5.23×10^5	38.62%
4	1.91×10^5	3.13×10^5	61.02%
5	1.31×10^5	2.22×10^5	59.01%
6	1.82×10^5	3.08×10^5	59.09%
7	1.09×10^5	1.60×10^5	68.13%
8	1.32×10^5	1.88×10^5	70.21%
9	1.02×10^5	1.67×10^5	61.08%
10	0.77×10^5	1.20×10^5	64.17%
Average	-	-	60.57%

4.5 Experimental Result

Although software-in-the-loop simulation test has an obvious evidence that above-mentioned control systems are appropriate for Maha hydraulic hybrid drive system, realistic application and real-life measurement are also supposed to be analyzed in entity.

The main purpose of experimental test was to validate and verify the working of control strategies instead of doing performance test such like acceleration test or fuel consumption test. There were some working conditions that had been selected for this measurement test. First and foremost, engine speed was downsized since the experimental vehicle were only driving in the parking lot around the lab and there are many speed bumps that it could not achieve high velocity and engine do not need to be running at very high speed at low velocity for saving fuel; therefore, the maximum velocity during this test was about 28 km/h. Secondly, the initial state of charge of high-pressure accumulator was around 270 bar. Last but not the least, control strategies for acceleration (hybrid mode and non-hybrid mode) along with braking (regenerative brake and friction brake with regenerative brake) and coasting were included, which were discussed in this section by means of the results of measurement data of forward operation. It should be mentioned that it is a driver-vehicle close-loop system with data acquisition, and pedal positions deriving from the action of driver are the merely input signals for the whole system.

In the bellowing figures from **Figure 4.34** to **Figure 4.37,** non-hybrid mode is represented by black block, hybrid mode is represented by green block, orang blocks show regenerative brake mode, red blocks show friction brake with regenerative brake, and only friction brake condition is represented by purple block. Following data containing pedal position, vehicle velocity, pressure inside the hydraulic system were obtained by all kinds of sensors and derived from data acquisition system, but displacements of all hydraulic units were command data in place of measurement data as a result of without displacement sensor. Besides, by reason of applying torque-based control algorithm for acceleration, even if in non-hybrid mode, secondary control was employed to control all displacements. Meanwhile, engine control was modified to fit this control method. Nevertheless, this dissertation is not contributed to secondary control as well as engine control, details about those control methods do not to be elaborated.

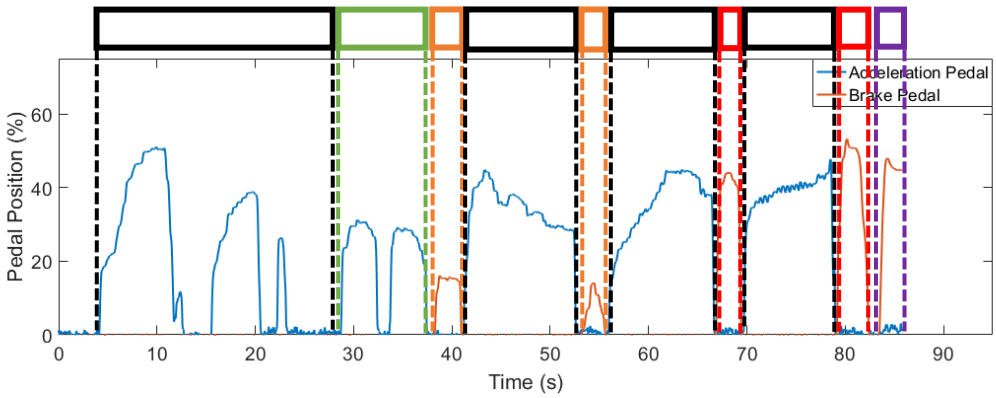

Figure 4.34: Measurement Data of Pedal Position

As acceleration pedal was pressed, displacement of unit 1, unit 2, unit 3 were commanded by acceleration controller to track desired torque according to its torque map corresponding to

pedal position. For the same reason in braking, brake controller needs to track commanded torque by changing displacements of hydraulic units but in this time displacement of unit 1 would be zero.

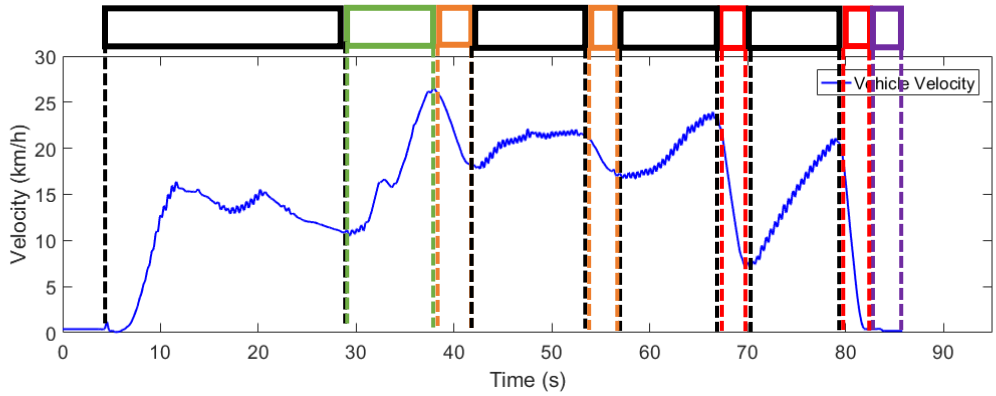

Figure 4.35: Measurement Data of vehicle Velocity

However, switching from non-hybrid mode to hybrid mode or inverse depended on supervisory control automatically. When all conditions were satisfied, system could work on hybrid mode, in other words, as long as one of the switching criteria inside supervisory control did not meet, energy stored in high-pressure accumulator would not be used. During the hybrid mode, the driver lifted his foot off the accelerator pedal for about 0.7 seconds, thus all the units come down to zero displacement during this time (since the vehicle is coasting), however the accelerator pedal was immediately pressed and the pressures go back up quickly. The vehicle kept on driving in the hybrid mode since the HPA was connected throughout this time.

For braking, regenerative brake can provide enough torque when driver only wanted to have a general braking event such as braking events around 40 second and 55 second. On the other hand, two relative hard braking events were shown from 68 to 70 second and 80 to 81 second respectively, whose friction brake was activated as well in order to provide extra torque to stop the vehicle. Friction brake only on final term after 85 second occurred because of zero vehicle velocity. In fact, during this term displacements of all units were still controlled by brake pedal instead of disabling supervisory control for brake. But it is a pity that without torque meter or displacement sensor (the diagram of displacements shown below is commanded displacement rather than real displacement measured by sensor) for measuring precise torque provided by hydraulic transmission, in experimental test, energy recovery rate as well as torque cannot be displayed.

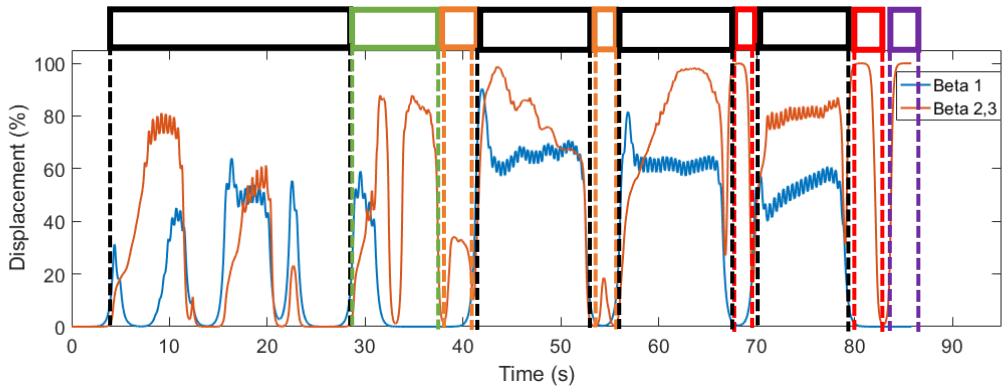

Figure 4.36: Measurement Data of Displacement

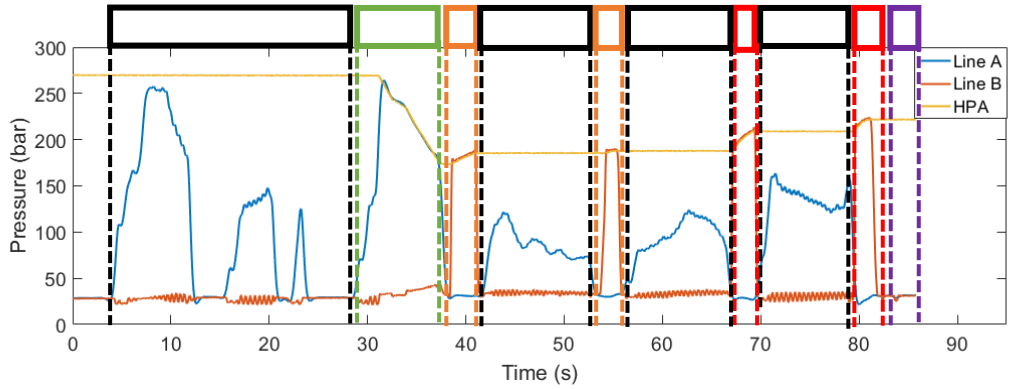

Figure 4.37: Measurement Data of Pressure

There appeared some oscillations of line B and displacements of all units in driving that should not have happened in the hydraulic hybrid transmission. After check and data analysis, it seems to be a fault with the low-pressure accumulator enabling valve and it keeps clicking while vehicle is driving, even though the controller is giving it OPEN command, which can be seed from **Figure 4.38**. It seems to be a physical fault and not for the controller. But a suitable filter is able to be employed to process data to flatten the oscillations without affecting the actual value to excess.

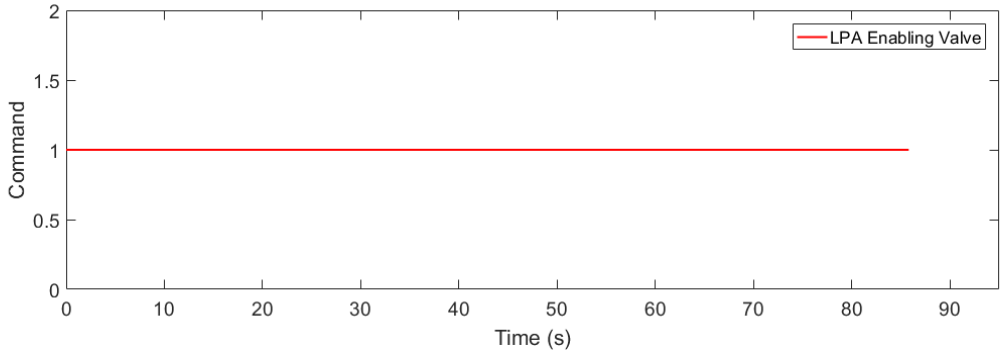

Figure 4.38: Command of LPA Enabling Valve

5. Summary and Future Work

The aim of this thesis was to develop novel control strategies on Maha hydraulic hybrid vehicle that was designed as a combination of a hydrostatic transmission and a series hybrid transmission implemented in an all-wheel-drive SUV with 4.0 L gas engine. This work started at doing investigation of the latest architecture as well as operating principle of this experimental vehicle. And then supporting simulation in MATLAB/SIMULINK environment had been built in order to validate new architecture and make preparation for design and verify toque-based control algorithms. Maha HHV had been developed in speed control while acceleration pedal position was related to desired vehicle speed and brake pedal position was proportional to displacements of unit 2 as well as unit 3 in previous research. Even though system worked as much as they desired, it also contained limitation and drawback, for instance, on each brake event, it had different brake feeling in same pedal travel because braking performance was always corresponding to state of charge of high pressure accumulator. Thus, new torque-based control algorithm was investigated. On the one hand, drivability and system performance should be same even better than conventional transmission through torque-based controller; on the other hand, it would be more reasonable and its driving experience would be close to present vehicle in the market that both acceleration and brake pedal are associated with desired torque.

Once orientation of new controller had been settled, a series of updates should be followed. First of all, an appropriate torque mapping as reference input associated with pedal position had been considered. It was based on the computation of original vehicle performance, hydraulic transmission characteristic, and driving comfort as well. To be continued, controller was designed to altered control value automatically along with system variables such as pressure, vehicle velocity. Feedback control logic should have been the preferred selection. However, neither displacement sensor or torque sensor were employed in vehicle, which were necessary for setting up a feedback loop. Therefore, a feedforward control method was applied to take place feedback logic. Thirdly, criteria for switching among hybrid mode and non-hybrid mode, refraining overheated problem as high-level control logic ought to change with respect to primary torque-based control system. Either acceleration condition assisted with energy stored in accumulator or full-charge of high pressure accumulator situation had been considered. Eventually, all control algorithms designed in this dissertation had been verified in simulation first, and then validated in real-life measurement by means of implementing all of control strategies through control and data acquisition system into Maha hydraulic hybrid vehicle. Although a physical fault of low-pressure accumulator enabling valve did lead to pressure ripple as well as oscillation of displacements during performing measurement, actual value did not determine significant effect thanks to suitable data processing technic.

An excess computation indicates that Maha hydraulic drive system has great potential in energy saving by downsizing its engine power shown in **Figure 5.1**. Blue curve shows instantaneous wheel power during whole UDDS drive cycle, whose power over zero is acceleration condition and below zero is regenerative brake. Red line represents a reduced engine power with wide open throttle. It can be noticed that even though engine has been downsized, available engine power is capable to meet the vast majority requirements of driving power profiting from the characteristic of continuously variable transmission as well as regenerative energy stored in accumulator. Meanwhile **Figure 5.2** clearly demonstrates that with increasing number of braking events, accessible energy in the whole system represented by yellow line rises up progressively owing to regenerative brake. The excess energy requirements shown in red curve are supposed to be compensated by practicable energy which

is captured through regenerative brake. Therefore, what we can predict is that available energy fully provided by engine at the beginning may be lower than requirement in some aggressive acceleration cases, which means system will need extra energy from other side to reach an aggressive acceleration rate; in other words, acceleration of the vehicle will be moderate in the first place only when less energy is saved in accumulator. This is the reason why available energy in the net is negative. But hydraulic hybrid is good at capturing braking energy as well as utilizing it. After several cycles, energy stored in accumulator will participate in prolusion system so that even engine has been downsized, prolusion system has the capability to provide enough power. All of overmentioned evidences prove that the same prolusion output power but with lower engine power and lower fuel consumption is able to be achieved by Maha hydraulic hybrid transmission.

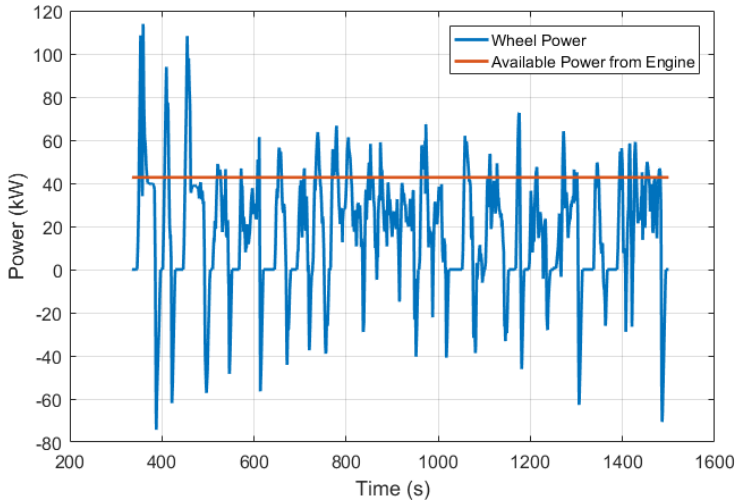

Figure 5.1: Power Relationship with Reduced Engine Power

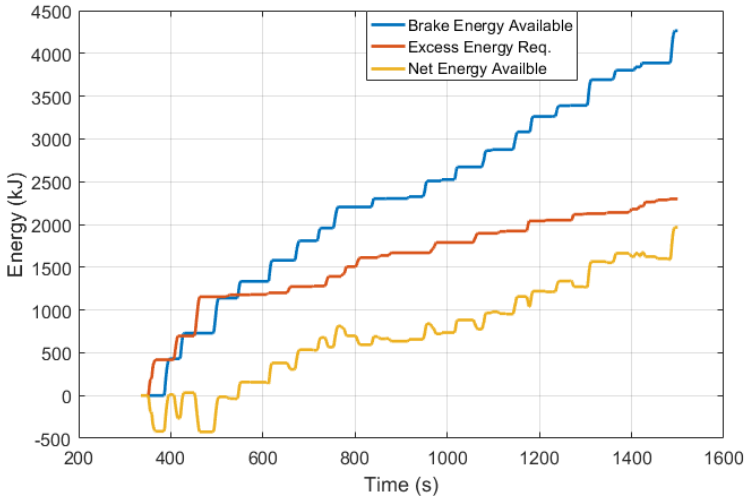

Figure 5.2: Energy Relationship with Reduced Engine Power

Commercializing Maha hydraulic hybrid transmission, additional work is required. First and foremost, functional safety features for electronic system applied in production on-road

automobiles must be satisfied with ISO 26262. Extra investigation including but not limit to identification of hazards, risk classification, definition of functional safety and safe state have to be explored to make corresponding changes in electronic system level. Moreover, fully electronic controlled brake pedal is capable of studying for improving drivability as well as braking performance when system operates on both regenerative braking and friction braking. Last but not the least, regardless of modified double-corner vehicle model has already met requirements of simulating hydraulic hybrid transmission, a more precise non-linear full or half vehicle model containing nonlinear deformation of the suspension as well as tyre, and side slip angle (both body slip angle and wheel slip angle) are able to investigated in future study for analyzing driving stability and more accuracy drive performance.

References

[1] Richard Folkson, "Introduction," in *Alternative fuels and advanced vehicle technologies for Improved Environmental Performance*.: Woodhead Publishing Limited, 2014, pp. 1-15.

[2] Administration, Energy Information. (2017) U.S.Energy Facts. [Online]. https://www.eia.gov/energyexplained/?page=us_energy_home#tab1

[3] Susan E. Williams, Robert G. Boundy Stacy C. Davis, "Petroleum," in *Transportation Energy Data Book Edition 35*.: U.S. Department of Energy, 2016, pp. 16-17.

[4] Victor Wouk, "Hybrids: then and now," *IEEE Spectrum*, vol. 32, no. 7, 1995.

[5] Tim Smith, Jeff Hopkins Mike Heskitt, "Design & Development of the LCO-140H Series Hydraulic Hybrid Low Floor Transit Bus: BUSolutions Final Technical Report," 2012.

[6] W Backe, "The present and future of fluid power," *Proceedings of the Institution of Mechanical Engineers, Part I: Journal of Systems and Control Engineering*, vol. 207, pp. 193-212, 1993.

[7] Rainer Resch Karl Th. Renius, "Continuously Variable Tractor Transmissions," in *Agricultural Equipment Technology Conference*, Louisville, 2005.

[8] Dan Edmunds. (2013, Oct.) What Are Hybrid Cars and How Do They Work? [Online]. https://www.edmunds.com/fuel-economy/what-is-a-hybrid-car-how-do-hybrids-work.html

[9] United States Environmental Protection Agency. (2007, Dec.) U.S. EPA demonstrates hydraulic hybrid UPS delivery vehicle: Vehicle achieves 60 – 70 percent better fuel economy, 40 percent lower greenhouse gas emissions. [Online]. https://www.epa.gov/cati/hydraulic-hybrid-vehicles

[10] Z. Filipi, "Hydraulic and pneumatic hybrid powertrains for improved fuel economy in vehicles," in *Alternative fuels and advanced vehicle technologies for Improved Environmental Performance*. Clemson: Woodhead Publishing Limited, 2014, p. 511.

[11] Manu Garg, "Regeratie Braking Mechanism," *International Journal of Engineering and Technical Research*, vol. 4, no. 2321-0869, pp. 152-153, 2016.

[12] Tri-Vien Vu Chih-Keng Chen, "Regenerative Braking Study For a Hydraulic Hybrid Vehicle," in *Proceedings of the 8th World Congress on Intelligent Control and Automation*, Taipei, 2011.

[13] Christine Ehret, Edward Greif and Markus G. Kliffken Simon Baseley, "Hydraulic Hybrid Systems for Commercial Vehicles," in *Commercial Vehicle Engineering Congress and Exhibition*, Rosemont, 2007.

[14] Y. ZhangC. -L. YinJ. -W. Zhang D. Peng, "Combined control of a regenerative braking and antilock braking system for hybrid electric vehicles," *International Journal of Automotive Technology*, vol. 9, no. 1976-3832, pp. 749-757, Dec. 2008.

[15] C. Lv, J. Gou, and D. Kong J. Zhang, "Cooperative control of regenerative braking and hydraulic braking of an electrified passenger car," *Proceedings of the Institution of Mechanical Engineers, Part D: Journal of Automobile Engineering*, vol. 226, no. 2041-2991 , pp. 1289-1302, Oct. 2012.

[16] Jincheng Zheng, Yongmao Su, and Jinghui Zhao Tao Liu, "A Study on Control Strategy of Regenerative Braking in the Hydraulic Hybrid Vehicle Based on ECE Regulations," *Mathematical Problems in Engineering*, vol. 2013, July 2013.

[17] Michael Sprengel and Monika Ivantysynova, "Novel transmission configuration fro hydraulic hybrid vehicles," in *Proceedings of the International Sci-Tech Conference "Machine Dynamics and Vibro Acoustics"*, Samara, 2012, pp. 207-209.

[18] Michael Sprengel and Monika Ivantysynova, "Investigation and Energetic Analysis of a Novel Hydraulic Hybrid Architecture for On-Road Vehicles," in *The 13th Scandinavian International Conference on Fluid Power*, Linköping, 2013, pp. 87-98.

[19] Michael Sprengel and Monika Ivantysynova, "Recent Developments in a Novel Blended Hydraulic Hybrid Transmission," in *SAE 2014 Commercial Vehicle Engineering Congress*, Rosemont, 2014.

[20] Michael Sprengel and Monika Ivantysynova, "Hardware-in-the-Loop Testing of a Novel Blended Hydraulic Hybrid Transmission," in *Proceedings of the 8th FPNI PhD Symposium*, Lappeenranta, 2014.

[21] Tyler J. Bleazard, "Hydraulic Hybrid Four Wheel Drive Sport Utility Vehicle - Utilizing the Blended Hybrid Architecture," Purdue University, Lafayette, Master Thesis 2015.

[22] Hiral Jayantilal Haria, "A Novel Mode-Swiching Hydraulic Hybrid for an On-Highway Vehicle: A Study of Architecture and Control," Purdue Universty, Lafayette, Master Thesis 2016.

[23] Mara Tanelli Sergio M. Savaresi, "Control-oriented Models of Braking," in *Active Braking Control Systems Design for Vehicles*. London, UK: Springer, 2010, ch. 2, pp. 17-52.

[24] Transportation Research Board, "Tires and Passenger Vehicle Fuel Economy: Informing Consumers, Improving Performance," Washington,D.C., Special Report 286 2006.

[25] D.Mikeska and M.Ivantysynova, "Virtual prototyping of power split drives," in *Proc. Bath Workshop on Power Transmission and Motion Control PTMC*, Bath,UK, 2002, pp. 95-111.

[26] Joshua D. Zimmerman, "Toward Optimal Multi-Actuator Displacement Controlled Mobile Hydraulic Systems," Purdue University, West Lafayette, Ph.D. Thesis 2012.

[27] HYDAC Technology GmbH. Bladder Accumulators Standard. [Online]. https://www.hydac.com.au/wp-content/uploads/2016/07/E.3.201.28.03.16.pdf

[28] F. Bauer, D. Feld M. Erkkilä, "Universal Energy Storage and Recovery System – A Novel Approach for Hydraulic Hybrid," in *The 13th Scandinavian International Conference on Fluid Power*, Linköping, 2013, pp. 45-52.

[29] Michael W. Sprengel, "Influence of Architecture Design on the Perfromance and Fuel Efficiency of Hydraulic Hybrid Transmissions," Purdue University, West Lafayette, Ph.D Thesis 2015.

[30] Prashant Shridhar Bokare Akhilesh Kumar Maurya, "Study of Deceleration Behaviour of Different Vehicle Types," *International Journal for Traffic and Transport Engineering,* vol. 2(3), no. 2217-544X, pp. 253-270, 2012.

[31] Bruce Francis, Allen Tannenbaum John Doyle, *Feedback Control Theory*.: Macmillan Publishing Co., 1990.

[32] Liang-Liang Xie and Lei Guo, "How much Uncertainty can be Dealt with by Feedback," *IEEE Transactions on Auomatic Control*, vol. 45, pp. 2203-2217, Dec. 2000.

[33] Arkadi Nemirovski, Alan J. Laub, Mahmoud Chilali Pascal Gahinet, *LMI Control Toolbox For Use with MATLAB*.: The MathWorks, Inc., 1995.

[34] Kiencke Uwe and Nielsen Lars, "PID Driver Model," in *Automotive Control Systems: for Engine, Driveline, and Vehicle*, 2nd ed.: Springer-Verlag Berlin Heidelberg, 2005, ch. 11.2, pp. 430-432.

[35] Baorui Chen, Biao MA, Man Chen Heyan LI, "Study on braking capacity of hydrostatic transmission vehicle," *IEEE Intelligent Vehicles Symposium*, vol. IV, pp. 848-851, June 2009.